Permutation-Based Noncoherent Space-Time Codes with Analog Energy Detection for IR-UWB Communications with PPM

Chadi Abou-Rjeily, *Senior Member IEEE*

***Abstract*—In this paper, we consider the problem of space-time (ST) coding for the noncoherent ultra-wideband (UWB) systems with pulse position modulation (PPM). In particular, we propose the first known family of ST codes that lends itself to optimal decoding with energy detectors. Energy detection avoids the sampling of the received signal where the sampling rates can be prohibitively high and escapes from the challenging task of estimating the dense multi-path UWB channel. In the absence of design criteria that are adapted to the problem under consideration, we derive two novel design criteria and propose the novel construction accordingly. The proposed code is based solely on permutations and hence it does not introduce any constellation expansion on the totally-real and unipolar PPM signal set. In other words, the components of the constructed codewords are limited to either zero or one indicating the absence or presence of an UWB pulse in the corresponding PPM slot, respectively. The above characteristics result in a remarked simplicity of the ST encoder/decoder making it an appealing solution to low-cost and low-power UWB systems. For a system equipped with n transmit antennas, we prove that the proposed code is capable of achieving a full transmit diversity order with M-PPM constellations for $M > n+1$ while transmitting at the rate of $\frac{1}{n}\log_2\binom{M-1}{n}$ bits per channel use.**

***Index Terms*—Ultra-Wideband (UWB), pulse position modulation (PPM), space-time, noncoherent, energy detection.**

I. Introduction and Problem Formulation

Recently, ultra-wideband (UWB) communications attracted significant attention as a competitive technology for short-range low-power wireless applications. Traditionally, UWB systems can be implemented with either coherent receivers, where the channel state information (CSI) is available at the receiver side, or with noncoherent receivers where the detection can be performed in the absence of CSI. Coherent UWB detection is based mainly on the conventional RAKE receivers where the arriving multi-path components are resolved and combined. However, given the very large number of multi-path components that follow from the high frequency-selectivity of the UWB channels, RAKE receivers having large number of fingers need to be implemented in order to capture a considerable portion of the signal energy thus rendering the channel estimation a challenging task [1], [2]. Moreover, typical signal processing involves sampling at least at the Nyquist rate which is in the order of several GHz for UWB signals. For the above reasons, the complexity of coherent UWB receivers can be prohibitive and noncoherent receivers were proposed as appealing cost-effective and low-power consumption alternatives. Communications over the noncoherent UWB channel can be realized with transmitted reference and differential schemes or with noncoherent energy detection receivers [3], [4]. The analysis and design of noncoherent UWB systems that are based on energy detection are well documented in the literature [5]–[9]. These systems are associated with M-ary pulse position modulation (PPM) where an UWB pulse is transmitted in one slot among the M available time slots. In this context, an energy detector collects the energies in the different time slots and decides in favor of the slot containing the maximum amount of energy [5]. The data rates that can be achieved by these systems were evaluated in [6] while robust and enhanced energy detection receivers that are capable of mitigating the noise effects were proposed and analyzed in [7]–[9].

On the other hand, information theoretic studies related to narrowband communications over Rayleigh channels showed that significant capacity gains can be achieved by multiple-input-multiple-output (MIMO) systems even when the CSI is not available to the transmitter and the receiver [10]. For the noncoherent narrowband MIMO channel, a popular strategy is to use unitary differential modulation [11], [12]. In the narrowband context, the literature on differential space-time (ST) coding is huge and dates back to more than a decade [11]–[17]. The various proposed codes include Cayley unitary ST codes [13], codes based on cyclic division algebras [14], codes optimized for given numbers of transmit antennas and rates [15], [16] and non-orthogonal codes with non-unitary constellations [17].

Recently, there was a growing interest in applying the ST coding techniques on impulse-radio (IR) UWB communications. The design of totally-real coherent ST codes that are tailored for UWB was addressed in [18]–[20]. On the other hand, the problem of noncoherent ST coding with UWB was considered in [21]–[27]. In particular, Alamouti-based [28] differential ST coding was considered in [21] for PPM constellations. In [22], a family of unitary and differential ST codes was proposed for M-PPM with any number of transmit antennas. [23], [24] proposed a differential scheme for IR-UWB with two transmit antennas and autocorrelation receivers. This scheme was associated with decision-feedback detection and sphere decoding in [25] and [26] in order to achieve improved performance levels and reduced decoding complexities, respectively. Finally, in [27], the pulse repetitions in time-hopping (TH) UWB systems were exploited

The author is with the Department of Electrical and Computer Engineering of the Lebanese American University (LAU), Byblos, Lebanon. (e-mail: chadi.abourjeily@lau.edu.lb).

for decoupling the data streams received from the different antennas in a simple and efficient way.

In this paper, we present a systematic method for constructing noncoherent ST codes that are suitable for IR-UWB with PPM and energy detection. The proposed construction possesses a large number of appealing features as follows.

- It is the first known noncoherent scheme that can be applied with analog energy detectors and for which the encoding/decoding is performed in a block-by-block basis. We will next shed more light on this property. The conventional baseband input-output relation of a MIMO channel can be written as: $\mathbf{Y_t} = \mathbf{H}\mathbf{X_t} + \mathbf{N_t}$ where t indexes the block channel use while $\mathbf{H}$, $\mathbf{Y_t}$ and $\mathbf{X_t}$ stand for the channel, decision and transmitted matrices, respectively. The existing coherent ST codes are based on decoding $\mathbf{X_t}$ following from the knowledge of $\mathbf{Y_t}$ and the channel matrix $\mathbf{H}$ whether in the context of narrowband or UWB communications (as in [18]–[20]). On the other hand, all of the existing noncoherent narrowband ST codes [11]–[17] and noncoherent IR-UWB ST codes [21]–[26] encode the data differentially in $\mathbf{X_t}$ and $\mathbf{X_{t-1}}$ while the receiver compares $\mathbf{Y_t}$ with $\mathbf{Y_{t-1}}$ for retrieving the value of the transmitted codeword without the knowledge of $\mathbf{H}$. While [21], [22] require the explicit knowledge of both $\mathbf{Y_t}$ and $\mathbf{Y_{t-1}}$, the detection in [23]–[26] is based on $\mathbf{Y_t}^H\mathbf{Y_{t-1}}$ ($[.]^H$ denotes the Hermitian transpose) where this quantity can be acquired by auto-correlating the signals received in the consecutive ST blocks. Unlike all the existing noncoherent ST codes, the detection associated with the proposed scheme can be accomplished from the unique knowledge of $\mathbf{Y_t}^H\mathbf{Y_t}$ whose diagonal elements correspond to the energies of the signals that fall on the receive antennas in different PPM time slots.

- The detection can be accomplished while bypassing all forms of involved sampling and analog-to-digital conversion (ADC). In fact, as indicated above, the detection is based on $\mathbf{Y_t}^H\mathbf{Y_t}$ (rather than $\mathbf{Y_t}$) and, hence, on the energies collected in the different PPM slots rather than the actual signals received in these slots. This constitutes an appealing feature since the sampling frequencies of the GHz UWB signals are prohibitively high. This feature is shared with the differential UWB solutions in [23]–[26] where the autocorrelation receivers can be implemented in the analog domain while the differential narrowband codes in [11]–[17] and the differential UWB codes in [21], [22] require the knowledge of the amplitudes and phases of the samples of the received signal.

- The proposed code can be applied with an arbitrary number of transmit antennas unlike [21], [23]–[26] that are limited to two transmit antennas.

- As all of the existing UWB coherent and noncoherent codes [18]–[27], the proposed code is totally-real and is thus suitable for real-valued carrier-less UWB transmissions where it is difficult to control the phases of the sub-nanosecond UWB pulses. In this context, it is worth noting that the narrowband noncoherent ST codes [11]–[17] are all complex-valued (based on phase rotations).

- In addition to being totally-real, the proposed ST code is shape-preserving and it does not introduce any constellation expansion on the PPM signal set. In other words, as in single-antenna systems, each antenna transmits only one unipolar pulse in one of the M available PPM slots; moreover, the pulses transmitted by the different antennas all have the same amplitude. This is an interesting feature that renders the complexity of the MIMO transmitter comparable to that of single-antenna transmitters where it is complicated to control the amplitude and phase of the very low duty-cycle sub-nanosecond UWB pulses. While the unipolarity constraint is respected by the UWB coherent code in [19] and the UWB differential code in [22], the UWB ST codes in [18], [20], [21], [23]–[27] are not unipolar. More specifically, while the proposed scheme transmits pulses that have the same amplitude, four amplitude levels are compelled by the differential code structure in [21] while the differential codes in [23]–[26] entail the transmission of bipolar pulses where the amplitudes of some of the transmitted pulses need to be inverted (for example, refer to eq. (1) in [24]). Moreover, the codes in [20], [23]–[26] are based on amplitude modulation and can not be applied with PPM.

- The ST decoding can be completely realized by linear operations that are based on additions thus avoiding the complex multiplication operations as will be highlighted later.

The above constraints can be relaxed by the high dimensionality of M-PPM signal sets (that are M-dimensional rather than two-dimensional as quadrature amplitude modulation (QAM) and phase shift keying (PSK)) resulting in an explicit code design capable of achieving high performance levels. First, we prove through a counter-example that the existing rank criterion [29] that was adopted for the design of the existing coherent [18]–[20] and noncoherent [11]–[17], [21]–[27] ST codes is not appropriate for the problem under consideration. In the absence of design criteria for the construction of noncoherent ST codes with energy detection, we propose two convenient design criteria and suggest a novel ST construction accordingly. In particular, the proposed construction takes the structure of the PPM signal set into consideration and it is based on associating permutation-based ST codewords that have a layered structure with a convenient unipolar constellation that is carved from the multidimensional PPM constellation.

The above features render the proposed scheme an appropriate low-cost solution for MIMO UWB systems. The advantages of the proposed solution compared to the existing noncoherent UWB ST codes in [21]–[27] can be summarized as follows. (i): The proposed code is the first known noncoherent scheme that can be applied with analog energy detectors. (ii): Unlike [21], [22], no ADC is required. (iii): Unlike [21], [23]–[27], the proposed scheme can be applied with any number of transmit antennas. (iv): Unlike [21], [23]–[27], the proposed code is unipolar and shape-preserving with PPM. (v): Unlike [23]–[26] that transmit at the fixed rate of 1 bit per channel use (bpcu), the proposed scheme transmits at the rate of $\frac{1}{n}\log_2\binom{M-1}{n}$ bpcu with M-PPM and n transmit antennas. (vi): Unlike [27], the proposed scheme can be applied in the absence of TH sequences.

II. SYSTEM MODEL

Consider a M-ary PPM constellation. A symbol of this M-dimensional constellation may be represented by a vector taken from the following set:

$$\mathcal{C}_{\text{PPM}} = \{\mathbf{e_m}\ ;\ m = 1, \ldots, M\}, \tag{1}$$

where $\mathbf{e_m}$ stands for the m-th column of the $M \times M$ identity matrix $\mathbf{I_M}$.

Consider a single-user MIMO-TH-UWB system where the transmitter and the receiver are equipped with P and Q antennas respectively. For ST codes that extend over J symbol durations, the signal transmitted from the p-th antenna can be written as:

$$s_p(t) = \sqrt{\frac{E_s}{P}} \sum_{j=1}^{J} \sum_{m=1}^{M} a_{p,m}^{(j)} w(t-(j-1)T_s-(m-1)\delta), \tag{2}$$

where $\mathbf{a_p^{(j)}} \triangleq [a_{p,1}^{(j)}, \ldots, a_{p,M}^{(j)}]^T \in \mathcal{C}_{\text{PPM}}$ is composed of $M-1$ zero components and one component that is equal to 1 corresponding to the position of the UWB pulse transmitted from the p-th antenna during the j-th symbol duration. In this case, the ST codeword can be represented by a $PM \times J$ matrix $\mathbf{C}$ whose $((p-1)M+m, j)$-th component is equal to $a_{p,m}^{(j)}$ for $p = 1, \ldots, P$, $m = 1, \ldots, M$ and $j = 1, \ldots, J$. In (2), $w(t)$ is the pulse waveform of duration T_w normalized to have unit energy, δ is the modulation delay and $T_s = M\delta$ is the symbol duration. E_s stands for the average energy per transmitted symbol and the normalizing factor $\frac{1}{\sqrt{P}}$ is introduced in order to have the same total transmitted energy as in the case of single-antenna systems.

A filtering operation is essential for the noncoherent scheme in order to limit the noise bandwidth and remove the out-of-band interference. After bandpass filtering, the filtered received signal at the q-th antenna can be written as:

$$r_q(t) = \sum_{p=1}^{P} \sum_{j=1}^{J} \sum_{m=1}^{M} a_{p,m}^{(j)} h_{q,p}(t-(j-1)T_s-(m-1)\delta) + \mathfrak{n}_q(t), \tag{3}$$

where $\mathfrak{n}_q(t)$ is the filtered additive white Gaussian noise (AWGN) at the q-th antenna with zero mean, single-sided power spectral density N_0 and single-sided bandwidth W. For notational simplicity, the multiplying factor $\sqrt{\frac{E_s}{P}}$ was removed from (2) since this term can be included in the expression of the noise variance. In this case, the variance of the noise term in (3) is equal to $\frac{PN_0}{2E_s}$. Finally, $h_{q,p}(t) = w(t) * g_{q,p}(t)$ where $*$ stands for convolution and $g_{q,p}(t)$ stands for the filtered impulse response of the frequency-selective channel between the p-th transmit antenna and the q-th receive antenna. For simplicity, the bandpass filter at the receiver front-end is assumed to be ideal with a single-sided bandwidth W. We denote by Γ the maximum delay spread of the UWB channel ($\Gamma \gg T_w$). In what follows, we assume that the MIMO-TH system is operating in the absence of Inter-Pulse-Interference (IPI). The IPI, that results from the interference between different PPM slots, can be eliminated by setting $\delta \geq \Gamma + T_w$.

The noncoherent receiver corresponds to a simple energy detector that collects the energy received within the different PPM time slots. This constitutes a low-complexity receiver that does not require any CSI neither at the transmitter nor at the receiver sides. We denote by $x_{j,m}$ the energy integrated within the m-th position of the j-th symbol duration for $m = 1, \ldots, M$ and $j = 1, \ldots, J$. This energy captured by the Q receive antennas is given by:

$$x_{j,m} = \sum_{q=1}^{Q} \int_0^{T_i} \left[r_q\left(t-(j-1)T_s-(m-1)\delta\right)\right]^2 \mathrm{d}t, \tag{4}$$

where T_i stands for the duration of the integration window. Note that the energy of the multi-path components decays exponentially with their corresponding arrival times in most of the widely approved UWB channel models [30]. Consequently, a compromise is often made on the choice of T_i where its value is restricted not to take very large values since at the tail of the channel impulse response the integrated noise energy might exceed the signal energy [8].

The decision at the output of the decoder is based uniquely on the MJ-dimensional decision vector $\mathbf{x}$ whose $((j-1)M+m)$-th component is equal to $x_{j,m}$ (the energy collected in the m-th PPM slot of the j-th symbol) given in (4) for $m = 1, \ldots, M$ and $j = 1, \ldots, J$:

$$\mathbf{x} = \left[\ x_{1,1} \ \cdots \ x_{1,M} \ \cdots\cdots \ x_{J,1} \ \cdots \ x_{J,M}\ \right]^T, \tag{5}$$

where $\mathbf{A}^T$ stands for the transpose of matrix $\mathbf{A}$.

III. ENCODER AND DECODER STRUCTURE

In what follows, we set $n = P$ and we consider minimal-delay ST codes for which $J = n$. The noncoherent scheme is based on the coherent shape-preserving PPM code proposed in [19] where, for M-dimensional PPM constellations, the structure for the $(PM \times J)$-dimensional codewords is given by:

$$\mathbf{C}(\mathbf{s}) = \begin{bmatrix} \mathbf{s_1} & \mathbf{s_2} & \cdots & \mathbf{s_n} \\ \mathbf{\Omega s_n} & \mathbf{s_1} & \ddots & \vdots \\ \vdots & \ddots & \ddots & \mathbf{s_2} \\ \mathbf{\Omega s_2} & \cdots & \mathbf{\Omega s_n} & \mathbf{s_1} \end{bmatrix} \ ; \ \mathbf{s} = [\mathbf{s_1}^T \ \cdots \ \mathbf{s_n}^T]^T, \tag{6}$$

where $\mathbf{s_1}, \ldots, \mathbf{s_n} \in \mathcal{C}_{\text{PPM}}$ given in (1) are the $(M \times 1)$-dimensional vector representations of the information symbols. $\mathbf{\Omega}$ is a $M \times M$ cyclic permutation matrix given by:

$$\mathbf{\Omega} = \begin{bmatrix} \mathbf{0_{1\times(M-1)}} & 1 \\ \mathbf{I_{M-1}} & \mathbf{0_{(M-1)\times 1}} \end{bmatrix}, \tag{7}$$

where $\mathbf{0_{m\times n}}$ is the all-zero $m \times n$ matrix.

In the context of coherent communications, $\mathbf{s} \in \mathcal{C}_{\text{PPM}}^n$ where there are no constraints on the selection of the symbols from the M-PPM signal set. In what follows, we will prove that the codewords in (6) are not suitable for noncoherent energy-based detection for $\mathbf{s} \in \mathcal{C}_{\text{PPM}}^n$. We will also prove that when $\mathbf{s}$ is bound to take values within a subset $\mathcal{C}$ of $\mathcal{C}_{\text{PPM}}^n$, then it would be possible to achieve a full diversity order. To summarize, the difference between the coherent and noncoherent scenarios resides in the choice of the set $\mathcal{C}$ and in the relation that needs to be satisfied between M and n for achieving full diversity.

The set $\mathcal{C}$ that will be associated with the codewords in (6) in the case of noncoherent energy detection has the following structure:

$$\mathcal{C} = \left\{ \mathbf{s} \mid \mathbf{s} = [\mathbf{e_{m_1}}^T \ \cdots \ \mathbf{e_{m_n}}^T]^T \ ; \ m_1 < m_2 < \cdots < m_n \ ; \ m_1, \ldots, m_n \in \{2, \ldots, M\} \right\}. \quad (8)$$

In other words, the PPM positions $m_1, \ldots, m_n$ of the transmitted symbols $\mathbf{s_1}, \ldots, \mathbf{s_n}$ in (6) are limited to take n distinct increasing values in the set $\{2, \ldots, M\}$. In Section IV, we justify this particular choice of the set $\mathcal{C}$.

The interest in maintaining the codeword structure given in (6) stems from the much desired property that this code is shape-preserving with PPM since $\mathbf{\Omega s_i} \in \mathcal{C}_{\text{PPM}}$ given in (1) whenever $\mathbf{s_i} \in \mathcal{C}_{\text{PPM}}$. In other words, the considered ST code does not introduce any constellation expansion on the original uncoded signal set. One can also identify the threaded structure of the codewords where encoded versions of $\mathbf{s_i}$ are transmitted on the $(i-1)$-th upper diagonal and $(n-(i-1))$-th lower diagonal. In this context, the multiplication of the elements of the lower triangular part of $\mathbf{C}(\mathbf{s})$ by $\mathbf{\Omega}$ resembles the multiplication by a non-norm element in the case of algebraic codes (for example [18]) and is introduced to meet the rank criterion [29].

Multiplying by the matrix $\mathbf{\Omega}$ in (7) defines a closed transformation over $\mathcal{C}_{\text{PPM}}$ where $\mathbf{\Omega e_m} = \mathbf{e_{m+1}}$ for $m = 1, \ldots, M-1$ and $\mathbf{\Omega e_M} = \mathbf{e_1}$. In this context, (6) and (7) are adapted to the structure of the PPM constellation where performing cyclic permutations, rather than multiplying by scalars or other forms of unitary matrices, restrains the encoded symbols to belong to $\mathcal{C}_{\text{PPM}}$. In other words, as in PPM single-antenna systems, exactly one unipolar UWB pulse is transmitted per symbol duration where no pulse combining/splitting, polarity inversion or amplitude scaling need to be performed thus keeping the complexity of the MIMO transmitter at its minimum. In fact, performing any of the above operations will considerably increase the transceivers' complexity given the very low duty-cycle of the UWB pulses.

From (8), the cardinality of $\mathcal{C}$ is equal to $\binom{M-1}{n}$. Since the proposed ST code extends over $J = n$ symbol durations, then this code transmits at the data rate of $R_{MIMO} = \frac{1}{J}\log_2\binom{M-1}{n}$ bpcu while the Single-Input-Single-Output (SISO) systems transmit at the rate of $R_{SISO} = \log_2 M$ bpcu. Consequently, the normalized data rate of the proposed scheme with respect to single-antenna systems is given by:

$$R = \frac{1}{n \log_2 M} \log_2 \binom{M-1}{n}. \quad (9)$$

Evidently, $R < 1$ and the proposed ST code results in a data rate reduction compared to single-antenna systems. Moreover, the implementation of the ST code is possible only if $M > n+1$. Finally, note that the proposed code is better suited for M-ary PPM with large values of M since R increases with M for a given value of n as shown in Fig. 1.

On the other hand, the Maximum-Likelihood (ML) detection associated with (6) corresponds to deciding in favor of the information vector $\hat{\mathbf{s}} = [\hat{\mathbf{s}}_1^T \ \cdots \ \hat{\mathbf{s}}_n^T]^T$ such that [5]:

$$\hat{\mathbf{s}} = \arg\max_{\mathbf{s}\in\mathcal{C}} \left[\mathbf{s}^T \mathbf{\Phi x}\right], \quad (10)$$

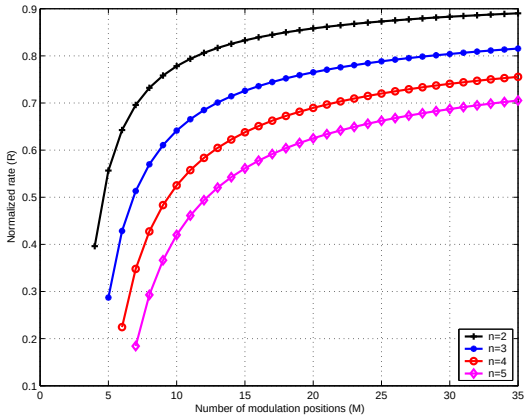

Fig. 1. The normalized rate in (9).

where the decision vector $\mathbf{x}$ is given in (5) while $\mathbf{\Phi}$ is the $nM \times nM$ matrix given by:

$$\mathbf{\Phi} = \begin{bmatrix} \mathbf{I_M} & \mathbf{I_M} & \cdots & \mathbf{I_M} \\ \mathbf{\Omega}^T & \mathbf{I_M} & \ddots & \vdots \\ \vdots & \ddots & \ddots & \mathbf{I_M} \\ \mathbf{\Omega}^T & \cdots & \Omega^T & \mathbf{I_M} \end{bmatrix}. \quad (11)$$

The decoding rule in (10) is analogous to the ML decision rule adopted in SISO noncoherent UWB systems deploying M-PPM [5] by observing that the transmitted UWB pulses occupy the positions determined by the nonzero components of the vector $\mathbf{s}^T\mathbf{\Phi}$.

Note that the components of $\mathbf{s}$ and $\mathbf{\Phi}$ can be equal to either 0 or 1. Consequently, the evaluation of the matrix product $\mathbf{s}^T\mathbf{\Phi x}$ in (10) corresponds to determining the summation of different combinations of elements of $\mathbf{x}$. Consequently, the implementation of (10) at the receiver does not require any multiplication operations. This significantly simplifies the ST decoding process that can be completely realized with adders. Evidently, despite the advantageous decoding complexity of the proposed scheme, this complexity remains higher than that of the orthogonal ST block codes (OSTBCs) [28]. However, OSTBCs require inverting the polarity of some of the transmitted pulses and are, hence, not shape-preserving with PPM. Moreover, OSTBCs are not suitable for energy detection where the imposed polarity inversion will be eradicated by this type of detection. The polarity inversion in OSTBCs is crucial for respecting the rank criterion and achieving full diversity and its suppression by energy detectors will result in reduced diversity orders. On the other hand, unlike OSTBCs, the proposed code can be applied with an arbitrary number of transmit antennas which constitutes an overwhelming advantage where the presented construction framework meets the challenging constraint of being generic. Finally, in the absence of CSI, OSTBCs are based on the conventional differential encoding/decoding approach while the proposed scheme can be applied on a block-by-block basis.

IV. Design Criteria and Diversity Order

A. Preliminaries and Motivating Example

In order to offer more insights on the choice of the set $\mathcal{C}$ in (8), we next consider the special case of $n = 2$ and $M = 4$. In this case, (8) can be written as:

$$\mathcal{C} \triangleq \mathcal{C}^{(2)} = \{\mathbf{s^{(1)}} = [\mathbf{e_2}^T \ \ \mathbf{e_3}^T]^T \ ; \ \mathbf{s^{(2)}} = [\mathbf{e_2}^T \ \ \mathbf{e_4}^T]^T \ ; \ \mathbf{s^{(3)}} = [\mathbf{e_3}^T \ \ \mathbf{e_4}^T]^T\}, \quad (12)$$

Consider also the following sets carved from $\mathcal{C}^2_{\text{PPM}}$:

$$\mathcal{C}^{(2)}_{\text{sub},1} = \mathcal{C}^{(2)} \cup \{\mathbf{s^{(4)}} = [\mathbf{e_1}^T \ \ \mathbf{e_2}^T]^T\} \ ; \quad (13)$$

$$\mathcal{C}^{(2)}_{\text{sub},2} = \mathcal{C}^{(2)} \cup \{\mathbf{s^{(5)}} = [\mathbf{e_1}^T \ \ \mathbf{e_4}^T]^T\}. \quad (14)$$

In [19] it was proven that, for all values of M, associating the codewords in (6) with the set $\mathcal{C}^2_{\text{PPM}}$ (of cardinality M^2) results in a full diversity order in the sense of satisfying the rank criterion [29] adopted for the construction of the existing coherent [18]–[20] and noncoherent [11]–[17] ST codes. More specifically, the unitary differential code design in [11]–[17] is based on maximizing the diversity product $\frac{1}{2}\min_{\mathbf{C(s)}\neq\mathbf{C(s')}} |\det(\mathbf{C(s)} - \mathbf{C(s')})|^{\frac{1}{n}}$. In this case, full diversity is achieved if the difference between any two codewords associated with non-identical pairs of elements of $\mathcal{C}^2_{\text{PPM}}$ has a full rank (of two); that is, $\det(\mathbf{C(s)} - \mathbf{C(s')}) \neq 0$ for $\mathbf{C(s)} \neq \mathbf{C(s')}$. Since the rank criterion is satisfied with the set $\mathcal{C}^2_{\text{PPM}}$, then it is also satisfied with the sets $\mathcal{C}^{(2)}$, $\mathcal{C}^{(2)}_{\text{sub},1}$ and $\mathcal{C}^{(2)}_{\text{sub},2}$ that are subsets of $\mathcal{C}^2_{\text{PPM}}$. In other words, according to the rank criterion [29], the three constructions obtained from associating (6) with $\mathcal{C}^{(2)}$, $\mathcal{C}^{(2)}_{\text{sub},1}$ and $\mathcal{C}^{(2)}_{\text{sub},2}$ are all expected to be fully diverse. However, these constructions exhibit very divergent performance trends as shown in Fig. 2 for $T_i = 2.5$ ns (details on the simulation setup are provided in section V). In particular, the construction with $\mathcal{C}^{(2)}_{\text{sub},2}$ manifests a performance with error floors while the construction with $\mathcal{C}^{(2)}_{\text{sub},1}$ does not enhance the diversity order where the corresponding error curve is parallel to that of single-antenna systems for large values of the signal-to-noise ratio (SNR). In this context, only the construction associated with $\mathcal{C}^{(2)}$ benefits from an enhanced diversity order [1]. The above example shows that the famous rank criterion is not suitable for noncoherent ST code design under the energy detectability constraint.

In what follows, we adopt the conventional approach of constructing ST codes for asymptotic values of the SNR [11]–[17]. In the absence of any design criterion for noncoherent ST codes with energy detection and PPM, we adopt the two following criteria for the selection of the set $\mathcal{C}$ to be associated with the codewords in (6).

B. Criterion 1

Criterion 1 [Interference Avoidance]: In order to avoid interference between the transmit antennas and ensure optimal energy decodability, at most one transmit antenna can be pulsed during each PPM time slot.

This criterion is intuitive and imposed by the structure of the receiver that is based on energy detection. In fact, the signals transmitted simultaneously by two or more transmit antennas within the same PPM slot add up incoherently at the receiver. In this case, the energy integrated within this slot might be small even in the case where the magnitudes of the corresponding channel coefficients are large. In the presence of noise, the energy collected during this PPM slot might be smaller than the energy integrated during the other slots (that do not contain any signals) resulting in erroneous decisions at the receiver even with low fading. Moreover, given that the receiver is based on energy detection, the pulses transmitted by two interfering transmit antennas can not be distinguished at the receiver side. For instance, for the example provided in subsection IV-A, the constructions with $\mathcal{C}^{(2)}$ and $\mathcal{C}^{(2)}_{\text{sub},1}$ satisfy criterion 1 while the construction with $\mathcal{C}^{(2)}_{\text{sub},2}$ does not satisfy this criterion since interference will occur in the first PPM slot of the first symbol duration when the symbol $\mathbf{s^{(5)}}$ in (14) is transmitted since the codeword takes the value $\mathbf{C}([\mathbf{e_1}^T \ \ \mathbf{e_4}^T]^T) = \begin{bmatrix} \mathbf{e_1} & \mathbf{e_4} \\ \mathbf{e_1} & \mathbf{e_1} \end{bmatrix}$ in this case.

Note that the existing noncoherent ST codes [11]–[14] do not necessarily satisfy criterion 1 since these codes are designed to be associated with receivers capable of reconstituting the amplitudes and phases of the received signals while this kind of information is not available at the output of energy detectors. Finally, associating these codes with energy detectors will result in a performance similar to that of the construction with $\mathcal{C}^{(2)}_{\text{sub},2}$ in Fig. 2.

Proposition 1: The proposed scheme, obtained from associating the codewords in (6) with the set $\mathcal{C}$ in (8), satisfies criterion 1.

Proof: In what follows an element $\mathbf{s}$ of $\mathcal{C}$ will be written as $\mathbf{s} = [\mathbf{s_1}^T \ \cdots \ \mathbf{s_n}^T]^T = [\mathbf{e_{m_1}}^T \ \cdots \ \mathbf{e_{m_n}}^T]^T$. From (6), it follows that the interference between the P transmit antennas can be eliminated over the J symbol durations if the M-

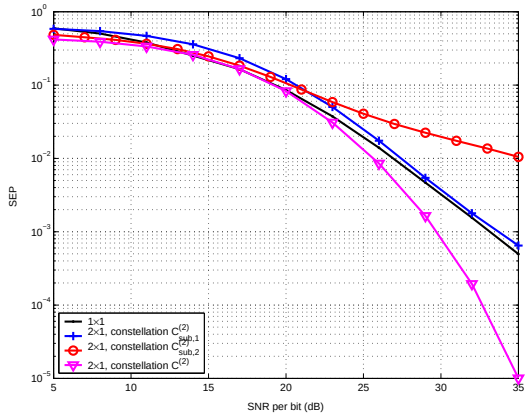

Fig. 2. Performance of the code in (6) with the constellations $\mathcal{C}^{(2)}$, $\mathcal{C}^{(2)}_{\text{sub},1}$ and $\mathcal{C}^{(2)}_{\text{sub},2}$ given in (12)-(14). Simulations are performed with 4-PPM and $T_i = 2.5$ ns.

[1]Note that the asymptotic error probability of fully-diverse $P \times Q$ MIMO systems over the IEEE 802.15.3a channel model does not scale as $\left(\frac{E_s}{N_0}\right)^{-PQ}$ as over Rayleigh channels (interested readers are referred to [31] and the references therein).

dimensional vectors $\mathbf{s_1},\ldots,\mathbf{s_n}$ satisfy the following relations:

$$\mathbf{s_i} \neq \mathbf{s_j} \;\; ; \;\; i,j=1,\ldots,n \; ; \; i \neq j, \tag{15}$$

$$\mathbf{\Omega s_i} \neq \mathbf{s_j} \;\; ; \;\; i=2,\ldots,n \; ; \; j=1,\ldots,i-1. \tag{16}$$

It is evident that the elements of $\mathcal{C}$ given in (8) satisfy (15) since the modulation positions $m_1,\ldots,m_n$ are distinct. On the other hand, the vector $\mathbf{\Omega s_i}$ in (16) can be written as: $\mathbf{\Omega s_i} = \mathbf{e}_{\pi(\mathbf{m_i})}$ where $\pi(.)$ stands for the cyclic permutation of order 1 given by:

$$\pi(k) = (k \mod M) + 1. \tag{17}$$

For $m_i < M$ where $i \in \{2,\ldots,n\}$, $\pi(m_i) = m_i + 1$ implying that $\pi(m_i) > m_i > m_j$ for $j = 1,\ldots,i-1$ where the last inequality follows from (8). Consequently, $\pi(m_i) \neq m_j$ and $\mathbf{\Omega s_i} = \mathbf{e}_{\pi(\mathbf{m_i})} \neq \mathbf{e_{m_j}} = \mathbf{s_j}$ implying that (16) is satisfied in this case. On the other hand, from (8), only m_n can be equal to M. In this case, $\pi(m_n) = 1$ and, consequently, $\pi(m_n) \neq m_j$ for $j = 1,\ldots,n-1$ and (16) is satisfied since $m_j \in \{2,\ldots,M\}$ for all values of j. As a conclusion, elements of $\mathcal{C}$ satisfy (15) and (16) implying that the proposed scheme satisfies criterion 1. ■

C. Asymptotic Pairwise Error Probability

For ST codes satisfying criterion 1 and in the absence of IPI, the decision vector $\mathbf{x}$ in (5) can be written as:

$$\mathbf{x} = \mathbf{C_0}(\mathbf{s})\mathbf{h} + \underbrace{\eta^{(\mathbf{sn})} + \eta^{(\mathbf{nn})}}_{\triangleq \eta}, \tag{18}$$

where $\mathbf{h}$ is the P-dimensional vector given by $\mathbf{h} = [h_1 \;\cdots\; h_P]^T$ where the scalar h_p stands for the energy captured by the Q receive antennas when only the p-th transmit antenna is pulsed:

$$h_p = \sum_{q=1}^{Q} \int_0^{T_i} h_{q,p}^2(t)\mathrm{d}t \quad ; \quad p = 1,\ldots,P, \tag{19}$$

while $\mathbf{C_0}(\mathbf{s})$ is the $(nM \times n)$-dimensional matrix given by:

$$\mathbf{C_0}(\mathbf{s}) = \begin{bmatrix} \mathbf{s_1} & \mathbf{\Omega s_n} & \cdots & \mathbf{\Omega s_2} \\ \mathbf{s_2} & \mathbf{s_1} & \ddots & \vdots \\ \vdots & \ddots & \ddots & \mathbf{\Omega s_n} \\ \mathbf{s_n} & \cdots & \mathbf{s_2} & \mathbf{s_1} \end{bmatrix} \;\; ; \;\; \mathbf{s} = [\mathbf{s_1}^T \;\cdots\; \mathbf{s_n}^T]^T. \tag{20}$$

In (18), $\eta^{(\mathbf{sn})}$ is the JM-dimensional noise vector that can be written under the following form: $\eta^{(\mathbf{sn})} = [\eta_{1,1}^{(sn)},\ldots,\eta_{1,M}^{(sn)} \;\cdots\; \eta_{J,1}^{(sn)},\ldots,\eta_{J,M}^{(sn)}]^T$ where $\eta_{j,m}^{(sn)}$ is the signal-cross-noise term collected in the m-th PPM slot of the j-th symbol duration:

$$\eta_{j,m}^{(sn)} = 2\sum_{q=1}^{Q} \int_0^{T_i} \left[\sum_{p=1}^{P} a_{p,m}^{(j)} h_{q,p}(t)\right] \times \mathfrak{n}_q(t-(j-1)T_s-(m-1)\delta)\mathrm{d}t, \tag{21}$$

where the summation $\sum_{p=1}^{P} a_{p,m}^{(j)} h_{q,p}(t)$ is either zero or contains only one nonzero term for ST codes satisfying criterion 1. In this case, $\eta^{(\mathbf{sn})}$ is a zero-mean Gaussian random vector whose autocorrelation matrix is given by:

$$\begin{aligned} \mathbf{R}_{\eta^{(\mathbf{sn})}} &= \mathrm{E}\left[\eta^{(\mathbf{sn})}[\eta^{(\mathbf{sn})}]^T\right] = 4\frac{PN_0}{2E_s}\mathrm{diag}\left(\mathbf{C_0}(\mathbf{s})\mathbf{h}\right) \\ &= 2\frac{PN_0}{E_s}\mathrm{diag}\left(\mathbf{C_0}(\mathbf{s})\mathbf{h}\right), \end{aligned} \tag{22}$$

where E[.] stands for the averaging operator while diag($\mathbf{x}$) is a diagonal matrix whose main diagonal is equal to the vector $\mathbf{x}$. The diagonal elements of $\mathbf{R}_{\eta^{(\mathbf{sn})}}$ can be equal to zero indicating that the corresponding signal-cross-noise term is zero (due to the absence of the signal).

In the same way, $\eta^{(\mathbf{nn})}$ in (18) is the noise-cross-noise vector that can be written as: $\eta^{(\mathbf{nn})} = [\eta_{1,1}^{(nn)},\ldots,\eta_{1,M}^{(nn)} \;\cdots\; \eta_{J,1}^{(nn)},\ldots,\eta_{J,M}^{(nn)}]^T$ where:

$$\eta_{j,m}^{(nn)} = \sum_{q=1}^{Q} \int_0^{T_i} \mathfrak{n}_q^2(t-(j-1)T_s-(m-1)\delta)\mathrm{d}t. \tag{23}$$

While $\eta^{(\mathbf{sn})}$ is Gaussian, $\eta^{(\mathbf{nn})}$ is not Gaussian. However, if the time-bandwidth product T_iW is large enough, the term in (23) can be approximated as Gaussian with variance $QT_iW\left[\frac{N_0P}{E_s}\right]^2$ [3], [5], [9], [32]. In this case, the components of the aggregate noise vector $\eta = \eta^{(\mathbf{sn})} + \eta^{(\mathbf{nn})}$ are uncorrelated Gaussian random variables with autocorrelation matrix:

$$\mathbf{R}_\eta = \mathrm{E}\left[\eta\eta^T\right] = \frac{2PN_0}{E_s}\mathrm{diag}\left(\mathbf{C_0}(\mathbf{s})\mathbf{h}\right) + \frac{QT_iWP^2N_0^2}{E_s^2}\mathbf{I_{nM}}. \tag{24}$$

From (10) and (18), the decision metric associated with a candidate vector $\mathbf{s}' = [\mathbf{s_1'}^T \;\cdots\; \mathbf{s_n'}^T]^T \in \mathcal{C}$ when the codeword $\mathbf{C}(\mathbf{s})$ is transmitted can be written as:

$$\mathbf{s'}^T\mathbf{\Phi x} = \underbrace{\mathbf{s'}^T\mathbf{\Phi C_0}(\mathbf{s})\mathbf{h}}_{\triangleq d(\mathbf{s}\rightarrow\mathbf{s'})} + \mathbf{s'}^T\mathbf{\Phi}\eta. \tag{25}$$

Proposition 2: For large SNR, the conditional pairwise symbol error probability (SEP) of associating (6) with a set $\mathcal{C}$ can be written as: $p_{e|\mathbf{h}} = \frac{1}{\binom{M-1}{n}} \sum_{\mathbf{s}\in\mathcal{C}} \sum_{\mathbf{s'}\in\mathcal{C}\setminus\{\mathbf{s}\}} p_{e|\mathbf{h}}(\mathbf{s}\rightarrow\mathbf{s}')$ where the probability of transmitting the codeword $\mathbf{C}(\mathbf{s})$ and deciding in favor of $\mathbf{C}(\mathbf{s}')$ is given by:

$$p_{e|\mathbf{h}}(\mathbf{s}\rightarrow\mathbf{s}') = Q\left(\sqrt{\frac{E_s}{2PN_0}[d(\mathbf{s}\rightarrow\mathbf{s}) - d(\mathbf{s}\rightarrow\mathbf{s}')]} \times \left[1 - \frac{QT_iWPN_0}{2E_s}\frac{\sum_{p=1}^{P}[d_p(\mathbf{s}\rightarrow\mathbf{s}) - d_p(\mathbf{s}\rightarrow\mathbf{s}')]}{d(\mathbf{s}\rightarrow\mathbf{s}) - d(\mathbf{s}\rightarrow\mathbf{s}')}\right]\right), \tag{26}$$

where for all values of $\mathbf{s}$ and $\mathbf{s}'$ satisfying criterion 1, $d(\mathbf{s}\rightarrow\mathbf{s}') = \mathbf{s'}^T\mathbf{\Phi C_0}(\mathbf{s})\mathbf{h}$ which stands for the signal-part of the decision variable in (25) can be written under the following form:

$$d(\mathbf{s}\rightarrow\mathbf{s}') = \sum_{p=1}^{P} d_p(\mathbf{s}\rightarrow\mathbf{s}')h_p \;\; | \;\; d_p(\mathbf{s}\rightarrow\mathbf{s}') \in \{0,\ldots,J\} \text{ for } p = 1,\ldots,P. \tag{27}$$

TABLE I
THE VALUES OF $d(\mathbf{s} \to \mathbf{s}')$ FOR THE CONSTRUCTIONS WITH $\mathcal{C}^{(2)}_{\text{sub},1} = \{\mathbf{s^{(1)}}, \mathbf{s^{(2)}}, \mathbf{s^{(3)}}, \mathbf{s^{(4)}}\}$ AND $\mathcal{C}^{(2)} = \{\mathbf{s^{(1)}}, \mathbf{s^{(2)}}, \mathbf{s^{(3)}}\}$

	$\mathbf{s}' = \mathbf{s^{(1)}}$	$\mathbf{s}' = \mathbf{s^{(2)}}$	$\mathbf{s}' = \mathbf{s^{(3)}}$	$\mathbf{s}' = \mathbf{s^{(4)}}$
$\mathbf{s} = \mathbf{s^{(1)}}$	$2h_1 + 2h_2$	$h_1 + h_2$	h_1	h_2
$\mathbf{s} = \mathbf{s^{(2)}}$	$h_1 + h_2$	$2h_1 + 2h_2$	$h_1 + h_2$	$2h_2$
$\mathbf{s} = \mathbf{s^{(3)}}$	h_2	$h_1 + h_2$	$2h_1 + 2h_2$	$h_1 + h_2$
$\mathbf{s} = \mathbf{s^{(4)}}$	h_1	$2h_1$	$h_1 + h_2$	$2h_1 + 2h_2$

In this case, $d(\mathbf{s} \to \mathbf{s}) = J \sum_{p=1}^{P} h_p$ implying that $d_p(\mathbf{s} \to \mathbf{s}) = J = n \ \forall \ p \in \{1, \ldots, P\}$. In (26), $Q(x) = \frac{1}{\sqrt{2\pi}} \int_x^\infty e^{-\frac{t^2}{2}} \mathrm{d}t$ is the Q-function.

Proof: The proof is provided in Appendix A. The proof follows from an asymptotic analysis at high SNR based on the Gaussian approximation of the noise vector η. ∎

As shown in Appendix A, the integer $d_p(\mathbf{s} \to \mathbf{s}')$ in (27) can be written as: $d_p(\mathbf{s} \to \mathbf{s}') = \sum_{j=1}^{J} d_{p,j}(\mathbf{s} \to \mathbf{s}')$ where $d_{p,j}(\mathbf{s} \to \mathbf{s}') \in \{0, 1\}$. Interpreting this result, the relation $d_{p,j}(\mathbf{s} \to \mathbf{s}') = 1$ (resp. $d_{p,j}(\mathbf{s} \to \mathbf{s}') = 0$) means that the energy of the pulse transmitted by the p-th antenna in the j-th symbol duration is included (resp. not included) in $d(\mathbf{s} \to \mathbf{s}')$. Consequently, $d_p(\mathbf{s} \to \mathbf{s}')$ stands for the number of pulses transmitted by the p-th antenna whose energies are included in $d(\mathbf{s} \to \mathbf{s}')$. Note that the smaller the value of $d(\mathbf{s} \to \mathbf{s}')$, the less probable it is to decide in favor of $\mathbf{s}'$ when the codeword $\mathbf{C}(\mathbf{s})$ is transmitted. For instance, for the example provided in subsection IV-A, the metrics $d(\mathbf{s} \to \mathbf{s}')$ associated with the set $\mathcal{C}^{(2)}_{\text{sub},1}$ in (13) are reported in Table I. The metrics associated with $\mathcal{C}^{(2)}$ in (12) can be obtained from the first three rows and first three columns of this table.

D. Criterion 2

Using the relation $Q(x) \leq \frac{1}{2} e^{-\frac{x^2}{2}}$, (26) can be upper-bounded by:

$$p_{e|\mathbf{h}}(\mathbf{s} \to \mathbf{s}') \leq \frac{1}{2} \exp\left(-\frac{E_s}{4PN_0} \left[[d(\mathbf{s} \to \mathbf{s}) - d(\mathbf{s} \to \mathbf{s}')] - \frac{QT_iWPN_0}{E_s} \sum_{p=1}^{P} [d_p(\mathbf{s} \to \mathbf{s}) - d_p(\mathbf{s} \to \mathbf{s}')] \right] \right), \quad (28)$$

where the above bound is tight for large values of the SNR $\frac{E_s}{N_0}$ and where the relation $(1+\epsilon)^x \approx 1 + x\epsilon$ was applied for $\epsilon \ll 1$. From (27), the last equation can be written under the following from:

$$p_{e|\mathbf{h}}(\mathbf{s} \to \mathbf{s}') \leq \frac{1}{2} \prod_{p=1}^{P} \exp\left(-\frac{E_s[n - d_p(\mathbf{s} \to \mathbf{s}')][h_p - QT_iWPN_0/E_s]}{4PN_0} \right). \quad (29)$$

Similar to (26) and (29), the conditional pairwise SEP of a Single-Input-Multiple-Output (SIMO) system composed of the p-th transmit antenna and the Q receive antennas can be written as:

$$p^{(\text{SIMO})}_{e|h_p} = Q\left(\sqrt{\frac{E_s h_p}{2N_0}} \left[1 - \frac{QT_iWPN_0}{2E_s h_p} \right] \right) \leq \frac{1}{2} \exp\left(-\frac{E_s[h_p - QT_iWPN_0/E_s]}{4N_0} \right), \quad (30)$$

which when integrated over the probability density function (pdf) $p(h_p)$ [2] of h_p results in:

$$p^{(\text{SIMO})}_e(E_s/N_0) \approx \frac{1}{2} \int_0^{+\infty} e^{-\frac{E_s[h_p - QT_iWPN_0/E_s]}{4N_0}} p(h_p) \mathrm{d}h_p. \quad (31)$$

Given that $h_1 \ldots, h_P$ are identically distributed then, independently from their specific distribution, from (29) and (31) the average pairwise SEP can be written as:

$$p_e(\mathbf{s} \to \mathbf{s}') \approx 2^{P-1} \prod_{p=1}^{P} p^{(\text{SIMO})}_e \left(\frac{E_s}{N_0} \left(1 - \frac{d_p(\mathbf{s} \to \mathbf{s}')}{n} \right) \right). \quad (32)$$

The second design criterion is inferred from (32) as follows.

Criterion 2 [Fully Diversity with Energy Detection]: For codewords having the structure in (6) where the symbols are carved from a set $\mathcal{C}$, full transmit diversity can be achieved if for every element $\mathbf{s}$ in $\mathcal{C}$ there is no other element $\mathbf{s}' \neq \mathbf{s}$ in $\mathcal{C}$ verifying the relation $d_p(\mathbf{s} \to \mathbf{s}') = n$ for any value of p in $\{1, \ldots, P\}$.

In fact, when the above criterion is satisfied, the term $1 - \frac{d_p(\mathbf{s} \to \mathbf{s}')}{n}$ in (32) will be different from zero for all values of $p \in \{1, \ldots, P\}$, $\mathbf{s} \in \mathcal{C}$ and $\mathbf{s}' \in \mathcal{C} \backslash \{\mathbf{s}\}$. Consequently, (32) can be written as the product of the error probabilities of all the P SIMO channels that constitute the MIMO channel implying that there will be a P-fold decrease in the error probability showing that the ST code will achieve the entire transmit diversity order of P. On the other hand, if criterion 2 is not satisfied, then at least one term $1 - \frac{d_p(\mathbf{s} \to \mathbf{s}')}{n}$ will be equal to zero implying that there will be at maximum a $(P-1)$-fold decrease in the SEP implying that the system did not exploit the full transmit diversity order.

As an example, for the constructions with $\mathcal{C}$ and $\mathcal{C}^{(2)}_{\text{sub},1}$ that both satisfy criterion 1, Table I shows that the construction with $\mathcal{C}$ satisfies criterion 2 while the construction with $\mathcal{C}^{(2)}_{\text{sub},1}$ does not satisfy this criterion since $d_1(\mathbf{s^{(4)}} \to \mathbf{s^{(2)}}) = 2$ and $d_2(\mathbf{s^{(2)}} \to \mathbf{s^{(4)}}) = 2$. This justifies the difference in the achieved diversity orders as was reported in Fig. 2. In fact, from Table I and (32), the average pairwise SEPs of these

[2] An exact expression of $p(h_p)$ over the IEEE 802.15.3a channel model is not available and various approximations were proposed in the literature (interested readers are referred to [31] and the references therein). However, this does not affect the presented analysis that holds for any distribution $p(h_p)$.

constructions are:

$$p_e^{(\mathcal{C})} = \frac{2}{3}\left[4\left[p_e^{(\text{SIMO})}\left(\frac{E_s}{2N_0}\right)\right]^2 + 2p_e^{(\text{SIMO})}\left(\frac{E_s}{2N_0}\right)p_e^{(\text{SIMO})}\left(\frac{E_s}{N_0}\right)\right], \quad (33)$$

$$p_e^{(\mathcal{C}_{\text{sub},1}^{(2)})} = \frac{2}{4}\left[6\left[p_e^{(\text{SIMO})}\left(\frac{E_s}{2N_0}\right)\right]^2 + 4p_e^{(\text{SIMO})}\left(\frac{E_s}{2N_0}\right)p_e^{(\text{SIMO})}\left(\frac{E_s}{N_0}\right) + 2\frac{1}{2}p_e^{(\text{SIMO})}\left(\frac{E_s}{N_0}\right)\right]. \quad (34)$$

Evidently, (33) reflects a two-fold decrease in the SEP while (34) behaves asymptotically as $p_e^{(\text{SIMO})}(E_s/N_0)$ indicating an asymptotic performance analogous to that of SIMO systems and hence a reduced diversity order as can be verified from Fig. 2.

E. The Proposed Scheme Satisfies Criterion 2

Going back to the general case, we present the following proposition that constitutes an important intermediate step in proving that the proposed scheme satisfies criterion 2.

Proposition 3: If $d_p(\mathbf{s} \rightarrow \mathbf{s}') = n$ for a certain value of p in $\{1, \ldots, P\}$, then the component vectors of $\mathbf{s} = [\mathbf{s_1}^T, \ldots, \mathbf{s_n}^T]^T$ and $\mathbf{s}' = [\mathbf{s'_1}^T, \ldots, \mathbf{s'_n}^T]^T$ must be related to each other by the following relation:

$$\mathbf{s_i} = \mathbf{\Omega}^{\gamma(i)}\mathbf{s'}_{f(i)} \quad ; \quad i = 1, \ldots, n, \quad (35)$$

where $\gamma(i) \in \{0, \pm 1\}$ for $i = 1, \ldots, n$ and $f(.)$ defines a one-to-one relation among the elements of the set $\{1, \ldots, n\}$.

Proof: The proof is provided in Appendix B. ∎

As an example, for $n = 2$ with $\mathbf{s} = [\mathbf{s_1}^T \ \ \mathbf{s_2}^T]^T$ and $\mathbf{s}' = [\mathbf{s'_1}^T \ \ \mathbf{s'_2}^T]^T$, $d_1(\mathbf{s} \rightarrow \mathbf{s}')$ or $d_2(\mathbf{s} \rightarrow \mathbf{s}')$ can be equal to 2 if $\mathbf{s}$ is equal to one of the columns of the following matrix:

$$\begin{bmatrix} \mathbf{s'_1} & \mathbf{\Omega}^{\pm 1}\mathbf{s'_1} & \mathbf{s'_1} & \mathbf{\Omega s'_1} & \mathbf{\Omega s'_1} & \mathbf{\Omega}^{-1}\mathbf{s'_1} & \mathbf{\Omega}^{-1}\mathbf{s'_1} & \mathbf{s'_2} \\ \mathbf{s'_2} & \mathbf{s'_2} & \mathbf{\Omega}^{\pm 1}\mathbf{s'_2} & \mathbf{\Omega s'_2} & \mathbf{\Omega}^{-1}\mathbf{s'_2} & \mathbf{\Omega s'_2} & \mathbf{\Omega}^{-1}\mathbf{s'_2} & \mathbf{s'_1} \\ \mathbf{\Omega}^{\pm 1}\mathbf{s'_2} & \mathbf{s'_2} & \mathbf{\Omega s'_2} & \mathbf{\Omega s'_2} & \mathbf{\Omega}^{-1}\mathbf{s'_2} & \mathbf{\Omega}^{-1}\mathbf{s'_2} & & \\ \mathbf{s'_1} & \mathbf{\Omega}^{\pm 1}\mathbf{s'_1} & \mathbf{\Omega s'_1} & \mathbf{\Omega}^{-1}\mathbf{s'_1} & \mathbf{\Omega s'_1} & \mathbf{\Omega}^{-1}\mathbf{s'_1} & & \end{bmatrix}, \quad (36)$$

where for the first seven columns of the above matrix the function $f(.)$ in (35) is defined by $f(1) = 1$ and $f(2) = 2$ while for the last seven columns this function is given by $f(1) = 2$ and $f(2) = 1$ (these are the two possible one-to-one relations over $\{1, 2\}$). Going one step further, we will prove in proposition 4 that only the first column of the matrix in (36) constitutes a valid solution that results in $d_1(\mathbf{s} \rightarrow \mathbf{s}') = 2$ or $d_2(\mathbf{s} \rightarrow \mathbf{s}') = 2$.

We use the result of proposition 3 to reach the following main result.

Proposition 4: $d_p(\mathbf{s} \rightarrow \mathbf{s}') = n$ for a certain value of p in $\{1, \ldots, P\}$ if and only if $\mathbf{s} = \mathbf{s}'$ implying that the proposed diversity scheme is fully diverse based on criterion 2.

Proof: This proposition states that for the proposed scheme where (6) is associated with (8), $\gamma(i)$ in (35) can only be equal to 0 for all values of i in $\{1, \ldots, n\}$ while $f(.)$ can only correspond to the identity mapping $f(i) = i$ for $i \in \{1, \ldots, n\}$. The proof is provided in Appendix C. ∎

As a conclusion, associating the codewords in (6) with the constellation in (8) permits to satisfy criteria 1 and 2 thus ensuring the possibility of noncoherent detection and the enhanced diversity order with energy detectors.

V. Simulations and results

Simulations are performed over the IEEE 802.15.3a channel model recommendation CM2 [30] where the PQ sub-channels between the transmit and receive arrays are generated independently. A Gaussian pulse with a duration of $T_w = 0.5$ ns is used. The maximum delay spread of the CM2 channels does not exceed $\Gamma = 100$ ns; consequently, we fix $\delta = 100$ ns for eliminating IPI. We employ an ideal bandpass filter with $W = 5$ GHz. The presented results show the variation of the SEP as a function of the SNR per bit which is equal to $\frac{E_s}{N_0 \log_2 M}$ for single-antenna systems and to $\frac{E_s}{N_0 R \log_2 M}$ for the proposed scheme where R is given in (9). This results in a fair comparison where the resulting data rate reduction translates into a SEP performance loss.

Fig. 3 shows the performance with different number of transmit antennas in the case where the receiver is equipped with one antenna. In this figure, we set $M = 12$ and $T_i = 2.5$ ns. The obtained results show the high performance levels and the enhanced diversity orders that can be achieved by the proposed construction for large values of the SNR. Note that the data rate reduction introduced by the proposed scheme results in a performance loss for small values of the SNR where the proposed code is outperformed by single-antenna systems. In general, the performance degrades as the number of transmit antennas n increases since the normalized rate R in (9) decreases with n for a fixed value of M.

Fig. 4 shows the impact of the integration time T_i on the achievable performance levels with 7-PPM. Results show that increasing the value of T_i does not always enhance the performance where these results accentuate on the existence of an optimal integration time beyond which the performance degrades as T_i increases. This follows from the fact that more noise is integrated when T_i increases while the multi-path components at the tail of the channel impulse response assume small values. Fig. 4 highlights on the superiority of the proposed scheme. For example, at a SNR of 27 dB, the best performance that can be achieved by single-antenna systems is 3×10^{-5}. When the proposed scheme is applied with two transmit antennas, the best SEP decreases to 6×10^{-7}. Results also reflect the dependence of the optimal integration time on the different system parameters. For example, at a SNR of 25 dB, the optimal T_i decreases from around 23 ns to around 19 ns as the number of transmit antennas increases from one to two.

Fig. 5 shows the variation of the SEP as a function of the bit rate for $n = 2$, $T_i = 3$ ns and a varying value of M. For single-antenna systems, the bit rate is equal to $\log_2(M)/(M\delta)$ while this quantity is equal to $R\log_2(M)/(M\delta)$ for the proposed scheme reflecting the data rate reduction by the factor R given in (9). Evidently, the error rate increases with the bit

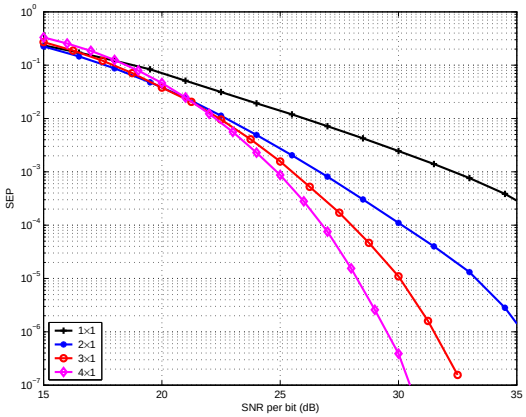

Fig. 3. Performance of $n \times 1$ TH-UWB systems with 12-PPM and $T_i = 2.5$ ns for $n = 1, \ldots, 4$.

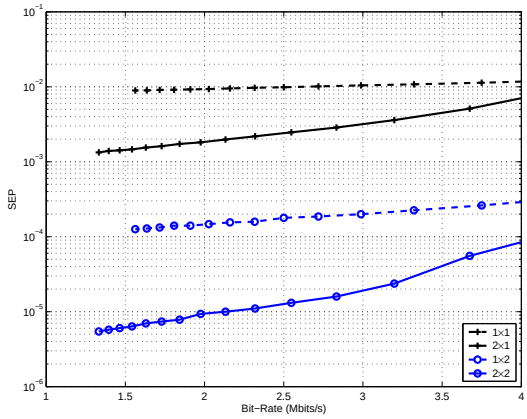

Fig. 5. Performance of the proposed scheme at a SNR of 25 dB with 1 and 2 receive antennas.

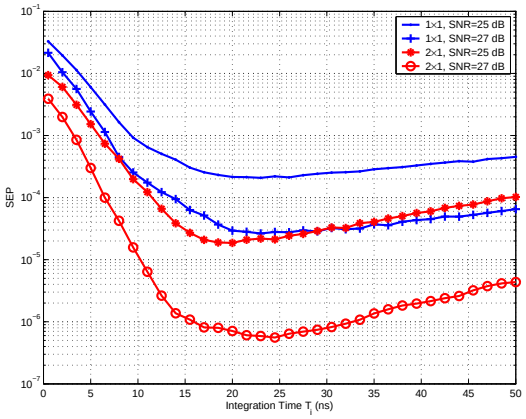

Fig. 4. Performance as a function of T_i with 7-PPM.

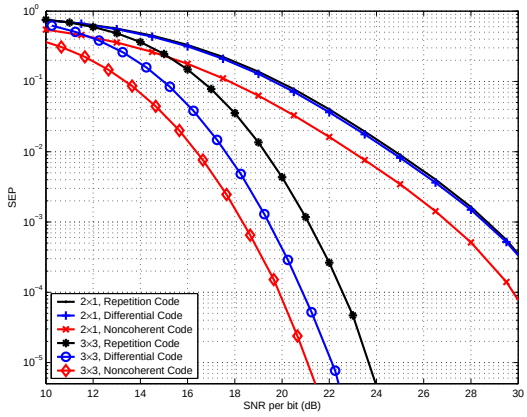

Fig. 6. Comparison between different codes with 10-PPM and $T_i = 3$ ns.

rate since any of these quantities can be compromised for the other. Results show the superiority of the proposed scheme especially at smaller bit rates where the SEP can be reduced by a factor that is around 100. In this context, it is worth noting that the SEPs of the proposed scheme increase at a faster pace because of the imposed data rate reduction that has as strong dependance on M.

Fig. 6 shows the performance of 2×1 and 3×3 MIMO systems where we compare different ST codes with 10-PPM and $T_i = 3$ ns. For the sake of fairness, the comparison is carried out between the codes that satisfy the stringent PPM shape-preserving constraint as follows. (i): The proposed noncoherent scheme that transmits at the rate of $\frac{1}{P}\log_2\binom{M-1}{P}$ which is equal to 2.585 bpcu and 2.131 bpcu for two and three transmit antennas, respectively. (ii): The differential ST code in [22] that transmits at the rate of $\frac{1}{P}\log_2(MP)$ which is equal to 2.161 bpcu for $P = 2$ and 1.635 bpcu for $P = 3$. (iii): The repetition code where the PPM symbols are transmitted separately by the P transmit antennas in P consecutive symbol durations while the noncoherent energy detector decides in favor of the slot with maximum energy. This code transmits at the rate of $\frac{1}{P}\log_2(M)$ which is equal to 1.661 bpcu and 1.107 bpcu for $P = 2$ and $P = 3$, respectively. Results show that all considered codes achieve the same diversity order where the corresponding SEP curves are practically parallel to each other for large values of the SNR. While the repetition code exhibits the poorest performance since it transmits at the lowest rate, results highlight the superiority of the proposed noncoherent code with respect to the differential code in [22]. In fact, while both codes satisfy the same construction constraints of being fully-diverse, real-valued, PPM shape-preserving and implementable in the absence of CSI, the main differentiating factor resides in the achievable rate (besides the different detection procedures). In this context, the noncoherent code achieves a higher rate that manifests in an improved performance since more information bits are included in each ST block for a given modulation order M while the codes respect equally the remaining design constraints. Compared to [22], results show performance gains of 1.5 dB and 1 dB for 2×1 and 3×3 systems, respectively.

While the assumption of channel independence might overestimate the performance gains and might not hold in some scenarios since it requires large antenna separations, Fig. 7 shows the applicability of the proposed scheme in real scenarios and highlights the impact of channel correlation. This figure shows the performance with 8-PPM and $T_i = 3$ ns over the space-variant UWB channel model proposed in [33]. Simulations are performed over profile 2 that corresponds to an office NLOS scenario for antenna array separations of 5 cm and 10 cm. Results show the high performance gains

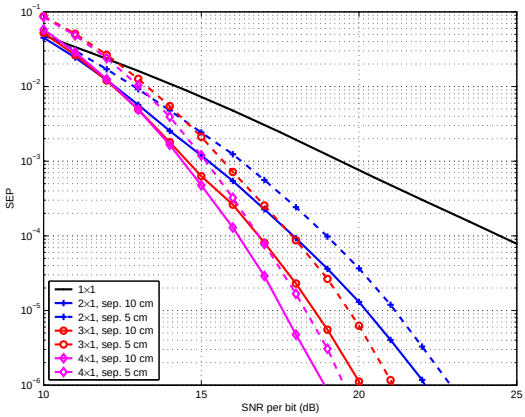

Fig. 7. Performance of 8-PPM over the Kunisch-Pamp profile-2 model [33].

over this realistic MIMO UWB channel model that takes spatial correlation into consideration. Despite the fact that the different channels are correlated, increasing the number of transmit antennas always enhances the performance especially for large values of the SNR. For example, a performance gain of 1.75 dB can be observed at 10^{-4} when the number of transmit antennas increases from 2 to 4 for an array separation of 10 cm.

VI. Conclusion

We have introduced a novel family of ST codes suited for noncoherent MIMO-UWB systems with energy detection. We have constructed this family of codes based on a new diversity criterion that guided us to the selection of a convenient multi-dimensional constellation capable of achieving a full diversity order when associated with the permutation-based codewords. The proposed scheme satisfies a large number of construction constraints without sacrificing its simplicity and hence its implementation results in important performance gains without inducing considerable complexity on the UWB transceiver circuitry. Future work needs to address suboptimal decoding to check whether the ML search can be limited to an appropriate subset of the codewords without drastically penalizing the performance.

Appendix A

We first determine the properties satisfied by $d(\mathbf{s}\rightarrow\mathbf{s}')$ in (25). Replacing the matrix $\mathbf{\Phi}$ by its value from (11) implies that $d(\mathbf{s}\rightarrow\mathbf{s}')$ can be written as:

$$d(\mathbf{s}\rightarrow\mathbf{s}')=\mathbf{s'}^{T}\mathbf{\Phi}\mathbf{C_0}(\mathbf{s})\mathbf{h}=[\mathbf{z}(\mathbf{s}')]^{T}\mathbf{C_0}(\mathbf{s})\mathbf{h}, \tag{37}$$

where $\mathbf{z}(\mathbf{s}')$ is the nM-dimensional vector given by:

$$\mathbf{z}(\mathbf{s}')=\mathbf{\Phi}^{T}\mathbf{s}'=\left[\begin{array}{ccc}[\mathbf{z_1}(\mathbf{s}')]^{T} & \cdots & [\mathbf{z_n}(\mathbf{s}')]^{T}\end{array}\right]^{T}, \tag{38}$$

where $\mathbf{z_1}(\mathbf{s}'),\ldots,\mathbf{z_n}(\mathbf{s}')$ are M-dimensional vectors given by:

$$\mathbf{z_{n'}}(\mathbf{s}')=\sum_{k=1}^{n'}\mathbf{s'_k}+\sum_{k=n'+1}^{n}\mathbf{\Omega}\mathbf{s'_k}\quad;\quad n'=1,\ldots,n. \tag{39}$$

Replacing equations (20) and (38)-(39) in (37) results in:

$$d(\mathbf{s}\rightarrow\mathbf{s}')=\sum_{p=1}^{P}h_p\sum_{j=1}^{J}d_{p,j}(\mathbf{s}\rightarrow\mathbf{s}')\triangleq\sum_{p=1}^{P}d_p(\mathbf{s}\rightarrow\mathbf{s}')h_p, \tag{40}$$

where:

$$d_{p,j}(\mathbf{s}\rightarrow\mathbf{s}')=\left\{\begin{array}{ll}[\mathbf{z_j}(\mathbf{s}')]^{T}\,\mathbf{\Omega}\mathbf{s_{n-p+j+1}} & \text{for}\ \ 1\leq j<p\\ [\mathbf{z_j}(s')]^{T}\,\mathbf{s_{j-p+1}} & \text{for}\ \ p\leq j\leq n\end{array}\right. . \tag{41}$$

Following from the interference avoidance conditions in (15) and (16), the vector $\mathbf{z_j}(\mathbf{s}')$ in (39) is equal to the sum of n distinct columns of the $M\times M$ identity matrix $\mathbf{I_M}$. Given that $n<M$ since the code is applied for $M>n+1$, then the components of $\mathbf{z_j}(\mathbf{s}')$ can be equal to either 0 or 1. On the other hand, given that the vectors $\mathbf{\Omega}\mathbf{s_{n-p+j+1}}$ and $\mathbf{s_{j-p+1}}$ in (41) are PPM vectors having $M-1$ zero components and one component that is equal to 1, then $d_{p,j}(\mathbf{s}\rightarrow\mathbf{s}')\in\{0,1\}$ for $p=1,\ldots,P$ and $j=1,\ldots,J$. From (40), $d_p(\mathbf{s}\rightarrow\mathbf{s}')=\sum_{j=1}^{J}d_{p,j}(\mathbf{s}\rightarrow\mathbf{s}')$ implying that $d_p(\mathbf{s}\rightarrow\mathbf{s}')\in\{0,\ldots,J\}$ completing the proof of (27). It is then straightforward to prove that $d_{p,j}(\mathbf{s}\rightarrow\mathbf{s})=1$ for all values of p and j implying that $d_p(\mathbf{s}\rightarrow\mathbf{s})=J=n\ \forall\ p\in\{1,\ldots,P\}$ resulting in $d(\mathbf{s}\rightarrow\mathbf{s})=n\sum_{p=1}^{P}h_p$.

We next prove (26) based on the conventional Gaussian approximation [3], [5], [9], [32]. From (10) and (25), the conditional pairwise error probability between $\mathbf{s}$ and $\mathbf{s}'$ can be written as:

$$p_{e|\mathbf{h}}(\mathbf{s}\rightarrow\mathbf{s}')=\Pr\left(\mathbf{s'}^{T}\mathbf{\Phi}\mathbf{x}\geq\mathbf{s}^{T}\mathbf{\Phi}\mathbf{x}\right), \tag{42}$$

$$=\Pr\left((\mathbf{s'}^{T}-\mathbf{s}^{T})\mathbf{\Phi}\eta\geq d(\mathbf{s}\rightarrow\mathbf{s})-d(\mathbf{s}\rightarrow\mathbf{s}')\right), \tag{43}$$

$$=\Pr\left([\mathbf{z}(\mathbf{s}')-\mathbf{z}(\mathbf{s})]^{T}\eta\geq d(\mathbf{s}\rightarrow\mathbf{s})-d(\mathbf{s}\rightarrow\mathbf{s}')\right), \tag{44}$$

where (38) was invoked in (44).

Given that each one of the vectors $\mathbf{z}(\mathbf{s}')$ and $\mathbf{z}(\mathbf{s})$ contains n^2 elements that are equal to 1 and $nM-n^2$ zero elements, then the components of $\mathbf{z}(\mathbf{s}')-\mathbf{z}(\mathbf{s})$ can be equal to 0, ±1 where the number of elements that are equal to 1 is the same as the number of elements that are equal to -1. Consequently, the Gaussian noise term $[\mathbf{z}(\mathbf{s}')-\mathbf{z}(\mathbf{s})]^{T}\eta$ has a zero mean.

On the other hand, the variance of the noise term in (44), that comprises the sum of uncorrelated Gaussian random variables, can be written as $\sigma^2=\sigma_1^2+\sigma_2^2$ where:

$$\sigma_1^2=\frac{2PN_0}{E_s}\left[\mathbf{z}(\mathbf{s}')-\mathbf{z}(\mathbf{s})\right]^{T}\left[\text{diag}\left(\mathbf{C_0}(\mathbf{s})\mathbf{h}\right)\right]\left[\mathbf{z}(\mathbf{s}')-\mathbf{z}(\mathbf{s})\right], \tag{45}$$

$$\sigma_2^2=\frac{QT_iWP^2N_0^2}{E_s^2}\left[\mathbf{z}(\mathbf{s}')-\mathbf{z}(\mathbf{s})\right]^{T}\left[\mathbf{z}(\mathbf{s}')-\mathbf{z}(\mathbf{s})\right], \tag{46}$$

where the result in (24) was invoked.

Now (45) can be written as:

$$\frac{\sigma_1^2E_s}{2PN_0}=\left(\left[\mathbf{z}(\mathbf{s}')-\mathbf{z}(\mathbf{s})\right]\circ\left[\mathbf{z}(\mathbf{s}')-\mathbf{z}(\mathbf{s})\right]\right)^{T}\mathbf{C_0}(\mathbf{s})\mathbf{h}, \tag{47}$$

where $\mathbf{A}\circ\mathbf{B}$ stands for the Hadamard element-wise product between matrices $\mathbf{A}$ and $\mathbf{B}$. As has been proven above,

elements of $\mathbf{z}(\mathbf{s}')-\mathbf{z}(\mathbf{s})$ belong to the set $\{0,\pm 1\}$. Since an element x of this set satisfies $x^2=|x|$, then (47) can be written as:

$$\frac{\sigma_1^2 E_s}{2PN_0}=|\mathbf{z}(\mathbf{s}')-\mathbf{z}(\mathbf{s})|^T\,\mathbf{C_0}(\mathbf{s})\mathbf{h}=\left|[\mathbf{z}(\mathbf{s}')-\mathbf{z}(\mathbf{s})]^T\mathbf{C_0}(\mathbf{s})\mathbf{h}\right|, \tag{48}$$

where the second equality follows since the elements of $\mathbf{C_0}(\mathbf{s})\mathbf{h}$ are nonnegative. From (37), the last equation can be written as:

$$\frac{\sigma_1^2 E_s}{2PN_0}=|d(\mathbf{s}\rightarrow\mathbf{s}')-d(\mathbf{s}\rightarrow\mathbf{s})|=d(\mathbf{s}\rightarrow\mathbf{s})-d(\mathbf{s}\rightarrow\mathbf{s}'), \tag{49}$$

where the second equality follows since $d(\mathbf{s}\rightarrow\mathbf{s}')\leq d(\mathbf{s}\rightarrow\mathbf{s})$.

On the other hand, (46) can be written as:

$$\frac{\sigma_2^2 E_s^2}{QT_iWP^2N_0^2}=2\left[n^2-[\mathbf{z}(\mathbf{s}')]^T\mathbf{z}(\mathbf{s})\right], \tag{50}$$

since $[\mathbf{z}(\mathbf{s}')]^T\mathbf{z}(\mathbf{s}')=[\mathbf{z}(\mathbf{s})]^T\mathbf{z}(\mathbf{s})=n^2$ since each one of the vectors $\mathbf{z}(\mathbf{s}')$ and $\mathbf{z}(\mathbf{s})$ contains exactly n^2 nonzero components that are equal to 1. On the other hand, from (20) and (38), the vector $\mathbf{z}(\mathbf{s})$ is related to the matrix $\mathbf{C_0}(\mathbf{s})$ by $\mathbf{z}(\mathbf{s})=\mathbf{C_0}(\mathbf{s})\mathbf{1_n}$ where $\mathbf{1_n}$ is the n-dimensional vector whose components are all equal to 1. Consequently, $[\mathbf{z}(\mathbf{s}')]^T\mathbf{z}(\mathbf{s})=[\mathbf{z}(\mathbf{s}')]^T\mathbf{C_0}(\mathbf{s})\mathbf{1_n}$. Comparing this relation with (37), we observe that the scalar $[\mathbf{z}(\mathbf{s}')]^T\mathbf{z}(\mathbf{s})$ can be obtained from $d(\mathbf{s}\rightarrow\mathbf{s}')$ by replacing $\mathbf{h}$ with $\mathbf{1_n}$ which from (40) results in $[\mathbf{z}(\mathbf{s}')]^T\mathbf{z}(\mathbf{s})=\sum_{p=1}^{P}d_p(\mathbf{s}\rightarrow\mathbf{s}')$. As a conclusion, (50) simplifies to:

$$\begin{aligned}\frac{\sigma_2^2 E_s^2}{QT_iWP^2N_0^2}&=2\left[n^2-\sum_{p=1}^{P}d_p(\mathbf{s}\rightarrow\mathbf{s}')\right]\\&=2\sum_{p=1}^{P}\left[d_p(\mathbf{s}\rightarrow\mathbf{s})-d_p(\mathbf{s}\rightarrow\mathbf{s}')\right],\end{aligned} \tag{51}$$

since $d_p(\mathbf{s}\rightarrow\mathbf{s})=n$ for $p=1,\ldots,P$.

Finally, (44) can be written as $p_{e|\mathbf{h}}(\mathbf{s}\rightarrow\mathbf{s}')=Q\left(\frac{d(\mathbf{s}\rightarrow\mathbf{s})-d(\mathbf{s}\rightarrow\mathbf{s}')}{\sqrt{\sigma_1^2+\sigma_2^2}}\right)$ where $Q(x)$ is the Q-function. Replacing σ_1 and σ_2 by their values from (49) and (51), respectively, results in:

$$p_{e|\mathbf{h}}(\mathbf{s}\rightarrow\mathbf{s}')=Q\left(\sqrt{\frac{E_s}{2PN_0}}\left[\frac{d(\mathbf{s}\rightarrow\mathbf{s})-d(\mathbf{s}\rightarrow\mathbf{s}')}{1+\frac{QT_iWPN_0}{E_s}\frac{\sum_{p=1}^{P}[d_p(\mathbf{s}\rightarrow\mathbf{s})-d_p(\mathbf{s}\rightarrow\mathbf{s}')]}{d(\mathbf{s}\rightarrow\mathbf{s})-d(\mathbf{s}\rightarrow\mathbf{s}')}}\right]^{\frac{1}{2}}\right). \tag{52}$$

Using the relation $(1+\epsilon)^n\approx 1+n\epsilon$ for $\epsilon\ll 1$, (52) tends asymptotically to (26) for large values of the SNR.

APPENDIX B

Proposition 3 implies that when $d_p(\mathbf{s}\rightarrow\mathbf{s}')=n$, then every element of $\{\mathbf{s_i}\}_{i=1}^n$ will be related to a unique element of $\{\mathbf{s'_{i'}}\}_{i'=1}^n$ by the relation $\mathbf{s_i}=\Omega^l\mathbf{s'_{i'}}$ where $l\in\{0,\pm 1\}$. In other words, no two ore more elements of the first set can be related to a single element of the second set and vice-versa. From (40), $d_p(\mathbf{s}\rightarrow\mathbf{s}')=n$ if and only if $d_{p,1}(\mathbf{s}\rightarrow\mathbf{s}')=\cdots=d_{p,J}(\mathbf{s}\rightarrow\mathbf{s}')=1$. From (39) and (41), the relation $d_{p,j}(\mathbf{s}\rightarrow\mathbf{s}')=1$ with $1\leq j<p$ implies that one of the following relations must be verified:

$$\exists k\in\{1,\ldots,j\}\ ;\ \mathbf{\Omega s_{n-p+j+1}}=\mathbf{s'_k}, \tag{53}$$

$$\exists k\in\{j+1,\ldots,n\}\ ;\ \mathbf{\Omega s_{n-p+j+1}}=\mathbf{\Omega s'_k}\Rightarrow\mathbf{s_{n-p+j+1}}=\mathbf{s'_k}. \tag{54}$$

In the same way, the relation $d_{p,j}(\mathbf{s}\rightarrow\mathbf{s}')=1$ with $p\leq j<n$ implies that one of the following relations must hold:

$$\exists k\in\{1,\ldots,j\}\ ;\ \mathbf{s_{j-p+1}}=\mathbf{s'_k}, \tag{55}$$

$$\exists k\in\{j+1,\ldots,n\}\ ;\ \mathbf{s_{j-p+1}}=\mathbf{\Omega s'_k}. \tag{56}$$

Equations (53)-(56) can be summarized in one equation that describes the implication of having $d_{p,j}(\mathbf{s}\rightarrow\mathbf{s}')=1$ as follows:

$$\mathbf{s_{g(j)}}=\mathbf{\Omega}^{\gamma(j)}\mathbf{s'_{k(j)}}, \tag{57}$$

where:

$$g(j)\triangleq n-p+j+1\ ;\ \gamma(j)\triangleq\begin{cases}-1, & k(j)\leq j;\\ 0, & k(j)>j.\end{cases}\quad\text{if } 1\leq j<p, \tag{58}$$

and:

$$g(j)\triangleq j-p+1\ ;\ \gamma(j)\triangleq\begin{cases}0, & k(j)\leq j;\\ 1, & k(j)>j.\end{cases}\quad\text{if } p\leq j<n. \tag{59}$$

We will next prove the following proposition that highlights the impact of having the two quantities $d_{p,j_1}(\mathbf{s}\rightarrow\mathbf{s}')$ and $d_{p,j_2}(\mathbf{s}\rightarrow\mathbf{s}')$ being equal to one simultaneously. The impact of having the $J=n$ quantities $\{d_{p,j}(\mathbf{s}\rightarrow\mathbf{s}')\}_{j=1}^n$ all equal to one will follow directly.

Proposition 5: For a given value of p in $\{1,\ldots,P\}$ and for the values of j_1 and j_2 satisfying $1\leq j_1<j_2\leq J$, $d_{p,j_1}(\mathbf{s}\rightarrow\mathbf{s}')=d_{p,j_2}(\mathbf{s}\rightarrow\mathbf{s}')=1$ if and only if two unique elements of $\{\mathbf{s_i}\}_{i=1}^n$ are related to other two unique elements of $\{\mathbf{s'_{i'}}\}_{i'=1}^n$ by:

$$\mathbf{s_{i_1}}=\Omega^{0,\pm1}\mathbf{s'_{i'_1}}\ ,\ \mathbf{s_{i_2}}=\Omega^{0,\pm1}\mathbf{s'_{i'_2}}\ \mid\ i_1\neq i_2\ ,\ i'_1\neq i'_2, \tag{60}$$

where, for simplicity of notation, $\Omega^{0,\pm1}$ stands for Ω^l for $l=0,\pm1$.

Proof: The proof revolves around showing that i_1 and i_2, on one hand, as well as i'_1 and i'_2, on the other hand, are unique. These four integers are related to j_1 and j_2 by $i_m=g(j_m)$ and $i'_m=k(j_m)$ for $m=1,2$ where (57) holds for j_1 and j_2. The following three cases arise.

Case 1: Assume that $j_1<j_2<p$. In this case, (58) holds for both j_1 and j_2. Evidently, $i_1=g(j_1)\neq g(j_2)=i_2$ since $j_1\neq j_2$. We will next prove that $i'_1=k(j_1)\neq k(j_2)=i'_2$ by contradiction where we show that the relation $i'_1=i'_2$ implies that the corresponding symbol pair will not belong to the constellation $\mathcal{C}$. The following four cases need to be considered depending on the values of $\gamma(j_1)$ and $\gamma(j_2)$.

Case 1.1: $\gamma(j_1)=\gamma(j_2)=-1$. In this case, $\mathbf{\Omega s_{i_1}}=\mathbf{s'_{i'_1}}$ and $\mathbf{\Omega s_{i_2}}=\mathbf{s'_{i'_2}}$ resulting in $\mathbf{s_{i_1}}=\mathbf{s_{i_2}}$ since it is assumed that $i'_1=i'_2$. Given that $\mathbf{s}\in\mathcal{C}$, then the interference avoidance condition in (15) implies that the relation $\mathbf{s_{i_1}}=\mathbf{s_{i_2}}$ can not hold since $i_1\neq i_2$. Consequently, i'_1 can not be equal to i'_2 in

this case. Case 1.2: $\gamma(j_1)=\gamma(j_2)=0$ resulting in $\mathbf{s_{i_1}}=\mathbf{s'_{i'_1}}=\mathbf{s'_{i'_2}}=\mathbf{s_{i_2}}$. Consequently, as in case 1.1, the relation $\mathbf{s_{i_1}}=\mathbf{s_{i_2}}$ can not hold implying that the assumption $i'_1=i'_2$ is not valid. Case 1.3: $\gamma(j_1)=0$ and $\gamma(j_2)=-1$ resulting in $\mathbf{\Omega s_{i_2}}=\mathbf{s_{i_1}}$ which is not possible since the proposed constellation satisfies (16) with $i_2>i_1$ since $j_2>j_1$. Case 1.4: $\gamma(j_1)=-1$ and $\gamma(j_2)=0$ resulting in $\mathbf{\Omega s_{i_1}}=\mathbf{s_{i_2}}$ which does not violate any one of the conditions in (15) and (16). However, in this case, i'_1 must belong to $\{1,\ldots,j_1\}$ while i'_2 must belong to $\{j_2+1,\ldots,n\}$. Therefore, i'_1 can not be equal to i'_2 since $j_1<j_2$.

Case 2: Assume that $p\leq j_1<j_2$. In this case, (59) holds for both j_1 and j_2. Evidently, $i_1=g(j_1)\neq g(j_2)=i_2$ since $j_1\neq j_2$. Adopting the same approach as in case 1, we first assume that $i'_1=i'_2$. If either $\gamma(j_1)=\gamma(j_2)=0$ or $\gamma(j_1)=\gamma(j_2)=1$, then $\mathbf{s_{i_1}}$ must be equal to $\mathbf{s_{i_2}}$ which is not possible from (15). Consequently, the assumption $i'_1=i'_2$ is wrong. If $\gamma(j_1)=1$ and $\gamma(j_2)=0$, then the relation $i'_1=i'_2$ implies that $\mathbf{s_{i_1}}=\mathbf{\Omega s'_{i'_1}}=\mathbf{\Omega s'_{i'_2}}=\mathbf{\Omega s_{i_2}}$ thus contradicting (16) since $i_2>i_1$ which follows from $j_2>j_1$. Finally, if $\gamma(j_1)=0$ and $\gamma(j_2)=1$, then i'_1 must belong to $\{1,\ldots,j_1\}$ while i'_2 must belong to $\{j_2+1,\ldots,n\}$ implying that $i'_1\neq i'_2$ since $j_1<j_2$.

Case 3: We now consider the case where $j_1<p\leq j_2$. In this case (58) holds for j_1 while (59) holds for j_2. In this case, $i_1=n-p+j_1+1$ and $i_2=j_2-p+1$ implying that $i_1-i_2=n-(j_2-j_1)$ which results in $i_1>i_2$ since $(j_2-j_1)\in\{1,\ldots,n-1\}$ for $j_1<j_2$. As in case 1 and case 2, we will show that the relation $i'_1=i'_2$ is not acceptable. Four cases are possible. The following cases arise. Case 3.1: $\gamma(j_1)=-1$ and $\gamma(j_2)=0$. In this case, $\mathbf{\Omega s_{i_1}}=\mathbf{s'_{i'_1}}=\mathbf{s'_{i'_2}}=\mathbf{s_{i_2}}$ resulting in $\mathbf{s_{i_2}}=\mathbf{\Omega s_{i_1}}$. From (16), elements of $\mathcal{C}$ can not satisfy this last relation since $i_1>i_2$. Case 3.2: $\gamma(j_1)=-1$ and $\gamma(j_2)=1$. In this case, i'_1 must belong to $\{1,\ldots,j_1\}$ while i'_2 must belong to $\{j_2+1,\ldots,n\}$ implying that $i'_1\neq i'_2$. Case 3.3: $\gamma(j_1)=\gamma(j_2)=0$. This case results in $\mathbf{s_{i_1}}=\mathbf{s_{i_2}}$ thus contradicting (15) since $i_1\neq i_2$. Case 3.4: $\gamma(j_1)=0$ and $\gamma(j_2)=1$. As in case 3.1, this results in $\mathbf{s_{i_2}}=\mathbf{\Omega s_{i_1}}$ which contradicts (16) since $i_1>i_2$ in case 3.

As a conclusion, $i_1\neq i_2$ and $i'_1\neq i'_2$ in all cases completing the proof of proposition 5. ∎

Finally, considering the quantities $\{d_{p,j}(\mathbf{s}\rightarrow\mathbf{s}')\}_{j=1}^{J}$ two-by-two (where are all these quantities are equal to one so that $d_p(\mathbf{s}\rightarrow\mathbf{s}')=n$) results in the following set of relations from (60):

$$\mathbf{s_{i_j}}=\Omega^{0,\pm1}\mathbf{s'_{i'_j}}\ ,\ j=1,\ldots,n\ \mid\ i_1\neq\cdots\neq i_n\ ,\ i'_1\neq\cdots\neq i'_n, \tag{61}$$

implying that the n integers $i_1,\ldots,i_n$ as well as the n integers $i'_1,\ldots,i'_n$ span the entire set $\{1,\ldots,n\}$. Setting $i_j=i\in\{1,\ldots,n\}$ implies that i'_j can be written as $i'_j=f(i)$ where $f(.)$ is a bijective function thus completing the proof of proposition 3.

APPENDIX C

The decision metric in (37) can be written in a more convenient way as:

$$d(\mathbf{s}\rightarrow\mathbf{s}')=\mathbf{h}^T\mathbf{Z}(\mathbf{s}')\mathbf{s}, \tag{62}$$

where $\mathbf{s}=[\mathbf{s_1}^T,\ldots,\mathbf{s_n}^T]^T$, $\mathbf{s}'=[\mathbf{s'_1}^T,\ldots,\mathbf{s'_n}^T]^T$ and $\mathbf{Z}(\mathbf{s}')$ is the $n\times nM$ matrix given by:

$$\mathbf{Z}(\mathbf{s}')=\begin{bmatrix}[\mathbf{z_1}(\mathbf{s}')]^T & [\mathbf{z_2}(\mathbf{s}')]^T & \cdots & [\mathbf{z_n}(\mathbf{s}')]^T\\ [\mathbf{z_2}(\mathbf{s}')]^T & \cdots & [\mathbf{z_{n-1}}(\mathbf{s}')]^T & [\mathbf{z_1}(\mathbf{s}')]^T\mathbf{\Omega}\\ \vdots & \vdots & \vdots & \vdots\\ [\mathbf{z_n}(\mathbf{s}')]^T & [\mathbf{z_1}(\mathbf{s}')]^T\mathbf{\Omega} & \cdots & [\mathbf{z_{n-1}}(\mathbf{s}')]^T\mathbf{\Omega}\end{bmatrix}. \tag{63}$$

The matrix $\mathbf{Z}(\mathbf{s}')$ will be written in an equivalent way that better highlights the dependence of this matrix on each of the vectors $\{\mathbf{s'_i}\}_{i=1}^{n}$. The dependence on $\mathbf{s'_i}$ will be described by a $nM\times nM$ matrix $\mathbf{T}^{(i)}$ that will be considered as a block matrix whose (k,l)-th element is a $M\times M$ matrix. In this context, the n'-th anti-diagonal is defined as the (k,l)-th elements satisfying $k+l=n'+1$ for $n'=1,\ldots,2n-1$.

From (39), $\mathbf{z_{n'}}(\mathbf{s}')$ (the transpose of $[\mathbf{z_{n'}}(\mathbf{s}')]^T$) and $\mathbf{\Omega}^{-1}\mathbf{z_{n'}}(\mathbf{s}')$ (the transpose of $[\mathbf{z_{n'}}(\mathbf{s}')]^T\mathbf{\Omega}$) can be written as ($n'=1,\ldots,n$):

$$\mathbf{z_{n'}}(\mathbf{s}')=\sum_{k=1}^{n'}\mathbf{s'_k}+\sum_{k=n'+1}^{n}\mathbf{\Omega s'_k}, \tag{64}$$

$$\mathbf{\Omega}^{-1}\mathbf{z_{n'}}(\mathbf{s}')=\sum_{k=1}^{n'}\mathbf{\Omega}^{-1}\mathbf{s'_k}+\sum_{k=n'+1}^{n}\mathbf{s'_k}. \tag{65}$$

Equation (64) shows that the dependance of $\mathbf{z_{n'}}(\mathbf{s}')$ on $\mathbf{s'_i}$ is described by the matrix $\mathbf{\Omega}$ for $n'<i$ and by the identity matrix $\mathbf{I_M}$ for $n'\geq i$. Since $\mathbf{z_{n'}}(\mathbf{s}')$ appears in the n'-th anti-diagonal in (63), then the anti-diagonals $1,\ldots,i-1$ of $\mathbf{T}^{(i)}$ will contain the matrix $\mathbf{\Omega}$ while the anti-diagonals $i,\ldots,n$ will contain the matrix $\mathbf{I_M}$. Similarly, (65) shows that the dependance of $\mathbf{\Omega}^{-1}\mathbf{z_{n'}}(\mathbf{s}')$ on $\mathbf{s'_i}$ is described by $\mathbf{I_M}$ for $n'<i$ and by $\mathbf{\Omega}^{-1}$ for $n'\geq i$. Since $\mathbf{\Omega}^{-1}\mathbf{z_{n'}}(\mathbf{s}')$ appears in the $(n+n')$-th anti-diagonal in (63), then the anti-diagonals $n+1,\ldots,n+i-1$ of $\mathbf{T}^{(i)}$ will contain $\mathbf{I_M}$ while the anti-diagonals $n+i,\ldots,2n-1$ will contain $\mathbf{\Omega}^{-1}$. Consequently, $\mathbf{T}^{(i)}$ can be constructed as follows:

$$\mathbf{T}^{(i)}_{k,l}=\begin{cases}\mathbf{\Omega}, & 1\leq(k+l-1)<i;\\ \mathbf{I_M}, & i\leq(k+l-1)<n+i;\\ \mathbf{\Omega}^{-1}, & n+i\leq(k+l-1)\leq 2n-1.\end{cases}, \tag{66}$$

which can be written in an equivalent way as:

$$\mathbf{T}^{(i)}=\sum_{j=1}^{i-1}(\mathbf{I^{(j)}}\otimes\mathbf{\Omega})+\sum_{j=i}^{n+i-1}(\mathbf{I^{(j)}}\otimes\mathbf{I_M})+\sum_{j=n+i}^{2n-1}(\mathbf{I^{(j)}}\otimes\mathbf{\Omega}^{-1}), \tag{67}$$

where $\otimes$ stands for the Kronecker product and $\mathbf{I^{(j)}}$ is defined as the $n\times n$ matrix whose (m,m')-th element is equal to 1 if $m+m'=j+1$ and equal to 0 otherwise.

For example, with $n=3$ transmit antennas:

$$\mathbf{T}^{(1)}=\begin{bmatrix}\mathbf{I_M} & \mathbf{I_M} & \mathbf{I_M}\\ \mathbf{I_M} & \mathbf{I_M} & \mathbf{\Omega}^{-1}\\ \mathbf{I_M} & \mathbf{\Omega}^{-1} & \mathbf{\Omega}^{-1}\end{bmatrix};\mathbf{T}^{(2)}=\begin{bmatrix}\mathbf{\Omega} & \mathbf{I_M} & \mathbf{I_M}\\ \mathbf{I_M} & \mathbf{I_M} & \mathbf{I_M}\\ \mathbf{I_M} & \mathbf{I_M} & \mathbf{\Omega}^{-1}\end{bmatrix}$$
$$;\ \mathbf{T}^{(3)}=\begin{bmatrix}\mathbf{\Omega} & \mathbf{\Omega} & \mathbf{I_M}\\ \mathbf{\Omega} & \mathbf{I_M} & \mathbf{I_M}\\ \mathbf{I_M} & \mathbf{I_M} & \mathbf{I_M}\end{bmatrix}. \tag{68}$$

Following from (63) and (67), equation (62) can be written as:

$$d(\mathbf{s} \rightarrow \mathbf{s}') = \mathbf{h}^T \left[\sum_{i=1}^{n} \left[\mathbf{T}^{(i)} \left(\mathbf{I_n} \otimes \mathbf{s}'_{\mathbf{i}} \right) \right]^T \right] \mathbf{s}. \quad (69)$$

In this context, the interest of the previous derivations that led to writing the metric $d(\mathbf{s} \rightarrow \mathbf{s}')$ under the form given in (69) resides in the fact that this form better describes the dependence between the elements of $\mathbf{s}$ and $\mathbf{s}'$. In particular, the dependence between $\mathbf{s}'_{\mathbf{i}}$ and $\mathbf{s_j}$ is determined by the j-th row of $\mathbf{T}^{(i)}$.

Assume that $d_p(\mathbf{s} \rightarrow \mathbf{s}') = n$ for a certain value of p in $\{1, \ldots, P\}$. In this case, proposition 3 implies that:

$$\exists\ i \in \{1, \ldots, n\} \ \mid \ \mathbf{s_i} = \mathbf{\Omega}^{\gamma(i)} \mathbf{s}'_{\mathbf{n}}\ ;\ \gamma(i) \in \{0, \pm 1\}, \quad (70)$$

$$\exists\ j \in \{1, \ldots, n\} \ \mid \ \mathbf{s_n} = \mathbf{\Omega}^{\gamma(n)} \mathbf{s}'_{\mathbf{j}}\ ;\ \gamma(n) \in \{0, \pm 1\}. \quad (71)$$

Proposition 6: Equations (70) and (71) can hold simultaneously if and only if $i = j = n$ and $\gamma(i) = \gamma(n) = 0$ resulting in $\mathbf{s_n} = \mathbf{s}'_{\mathbf{n}}$.

Proof: Equation (67) shows that none of the elements of $\mathbf{T}^{(n)}$ is equal to $\mathbf{\Omega}^{-1}$. Consequently, $\gamma(i)$ in (70) can not be equal to -1. Similarly, elements of the n-th rows of $\mathbf{T}^{(1)}, \ldots, \mathbf{T}^{(n)}$ can be equal to either $\mathbf{I_M}$ or $\mathbf{\Omega}^{-1}$ implying that $\gamma(n)$ in (71) can not be equal to 1. Therefore, (70)-(71) can be written as:

$$\mathbf{s_i} = \mathbf{\Omega}^{\gamma(i)} \mathbf{s}'_{\mathbf{n}}\ ,\ \gamma(i) \in \{0, 1\}, \quad (72)$$

$$\mathbf{s_n} = \mathbf{\Omega}^{\gamma(n)} \mathbf{s}'_{\mathbf{j}}\ ,\ \gamma(n) \in \{0, -1\}. \quad (73)$$

In what follows, we set $\mathbf{s_p} = \mathbf{e_{m_p}}$ and $\mathbf{s}'_{\mathbf{p}} = \mathbf{e_{m'_p}}$ for $p = 1, \ldots, n$. The following cases need to be considered in order to prove that $m_n = m'_n$.

Case 1: assume that $m'_n = M$. In this case, $\gamma(i)$ in (72) must be equal to 0 since $\gamma(i) = 1 \Rightarrow \mathbf{e_{m_i}} = \mathbf{\Omega}^1 \mathbf{e_M} = \mathbf{e_1}$ which does not belong to the constellation given in (8). Consequently, $\gamma(i) = 0$ implying that $\mathbf{e_{m_i}} = \mathbf{e_M}$ implying that $i = n$ since, from (8), only $\mathbf{s_n}$ can occupy the M-th position. Therefore, $m_i = m_n = M = m'_n$ and $\mathbf{s_n} = \mathbf{s}'_{\mathbf{n}}$ in this first case.

Case 2: assume that $m'_n \neq M$. In this case, (72) implies that $m_i \in \{m'_n, m'_n + 1\} \Rightarrow m'_n \leq m_i$ and $m_n \in \{m'_j, m'_j - 1\} \Rightarrow m_n \leq m'_j$. On the other hand, from the constellation structure in (8), $m'_j \leq m'_n$ since $j \leq n$ and $m_i \leq m_n$ since $i \leq n$. Combining the obtained four inequalities results in: $m'_j \leq m'_n \leq m_i \leq m_n \leq m'_j$ which can be satisfied only when $m'_j = m'_n = m_i = m_n$ implying that $m_n = m'_n$ and $\mathbf{s_n} = \mathbf{s}'_{\mathbf{n}}$.

As a conclusion, in both cases, the relation $d_p(\mathbf{s} \rightarrow \mathbf{s}') = n$ can hold if and only if $\mathbf{s_n} = \mathbf{s}'_{\mathbf{n}}$. ■

In what follows, we will prove by recursion that $\mathbf{s_i} = \mathbf{s}'_{\mathbf{i}}$ starting with the value $i = n - 1$ and ending with $i = 1$. In other words, we assume that $\mathbf{s_j} = \mathbf{s}'_{\mathbf{j}}$ for $j = i + 1, \ldots, n$ and prove that this results in $\mathbf{s_i} = \mathbf{s}'_{\mathbf{i}}$. From what preceded, this recursion holds for $i = n$.

From proposition 3, $d_p(\mathbf{s} \rightarrow \mathbf{s}') = n$ implies that:

$$\exists\ j \in \{1, \ldots, i\} \ \mid \ \mathbf{s_j} = \mathbf{\Omega}^{\gamma(j)} \mathbf{s}'_{\mathbf{i}}\ ;\ \gamma(j) \in \{0, \pm 1\}, \quad (74)$$

$$\exists\ k \in \{1, \ldots, i\} \ \mid \ \mathbf{s_i} = \mathbf{\Omega}^{\gamma(i)} \mathbf{s}'_{\mathbf{k}}\ ;\ \gamma(i) \in \{0, \pm 1\}, \quad (75)$$

where j and k can not belong to $\{i+1, \ldots, n\}$ since $\mathbf{s_j} = \mathbf{s}'_{\mathbf{j}}$ for $j = i+1, \ldots, n$ and the function $f(.)$ in (35) is bijective.

We will next prove that (74) and (75) can hold only for $j = k = i$ and $\gamma(j) = \gamma(i) = 0$ implying that $\mathbf{s_i} = \mathbf{s}'_{\mathbf{i}}$. When removing the columns $i+1, \ldots, n$ of $\mathbf{T}^{(i)}$, (67) implies that only the matrices $\mathbf{I_M}$ and $\mathbf{\Omega}$ will remain in the expression of $\mathbf{T}^{(i)}$ and, consequently, $\gamma(j) \in \{0, 1\}$ in (74). Similarly, from (67), $\mathbf{\Omega}$ does not appear in the i-th row of the matrix $\mathbf{T}^{'(k)}$ obtained by removing the columns $i+1, \ldots, n$ of $\mathbf{T}^{(k)}$ for $k = 1, \ldots, i$. Consequently, $\gamma(i) \in \{0, -1\}$ in (75). Therefore, (74)-(75) simplify to:

$$\mathbf{s_j} = \mathbf{\Omega}^{\gamma(j)} \mathbf{s}'_{\mathbf{i}}\ ,\ \gamma(j) \in \{0, 1\}, \quad (76)$$

$$\mathbf{s_i} = \mathbf{\Omega}^{\gamma(i)} \mathbf{s}'_{\mathbf{k}}\ ,\ \gamma(i) \in \{0, -1\}. \quad (77)$$

As in the proof of proposition 6, we write $\mathbf{s_p} = \mathbf{e_{m_p}}$ and $\mathbf{s}'_{\mathbf{p}} = \mathbf{e_{m'_p}}$ for $p = 1, \ldots, n$ and prove that $m_i = m'_i$.

Since $m'_i \neq M$ because $i < n$, (76) results in $m_j \in \{m'_i, m'_i + 1\} \Rightarrow m'_i \leq m_j$ and $m_i \in \{m'_k, m'_k - 1\} \Rightarrow m_i \leq m'_k$. From (8), $m_j \leq m_i$ since $j \leq i$ and $m'_k \leq m'_i$ since $k \leq i$. Therefore, $m'_k \leq m'_i \leq m_j \leq m_i \leq m'_k$ which can only hold only when $m_i = m'_i$ implying that $\mathbf{s_i} = \mathbf{s}'_{\mathbf{i}}$.

As a conclusion, the relation $d_p(\mathbf{s} \rightarrow \mathbf{s}') = n$ can hold if and only if $\mathbf{s_i} = \mathbf{s}'_{\mathbf{i}}$ for $i = n, \ldots, 1$ completing the proof of proposition 4.

REFERENCES

[1] V. Lottici, A. N. D'Andrea, and U. Mengali, "Channel estimation for ultra-wideband communications," *IEEE J. Select. Areas Commun.*, vol. 20, no. 9, pp. 1638–1645, Dec. 2002.

[2] M. Z. Win and R. A. Scholtz, "On the energy capture of ultrawide bandwidth signals in dense multipath environments," *IEEE Commun. Lett.*, vol. 2, no. 9, pp. 245–247, Sep. 1998.

[3] J. D. Choi and W. E. Stark, "Performance of ultra-wideband communications with suboptimal receivers in multipath channels," *IEEE J. Select. Areas Commun.*, vol. 20, no. 9, pp. 1754–1766, Dec. 2002.

[4] Y. Chao and R. A. Scholtz, "Optimal and suboptimal receivers for ultra-wideband transmitted reference systems," in *Proc. IEEE Global Commun. Conf., San Francisco USA*, vol. 6, Dec. 2003, pp. 759–763.

[5] C. Carbonelli and U. Mengali, "M-PPM noncoherent receivers for UWB applications," *IEEE Trans. Wireless Commun.*, vol. 5, no. 8, pp. 2285–2294, Aug. 2006.

[6] Y. Souilmi and R. Knopp, "On the achievable rates of ultra-wideband PPM with non-coherent detection in multipath environments," in *Proc. IEEE Int. Conf. on Commun., Alaska USA*, vol. 5, 2003, pp. 3530–3534.

[7] A. A. D'Amico, U. Mengali, and E. A. de Reyna, "Energy-detection UWB receivers with multiple energy measurements," *IEEE Trans. Wireless Commun.*, vol. 6, no. 7, pp. 2652–2659, July 2007.

[8] F. Wang, Z. Tian, and B. M. Sadler, "Weighted energy-detection for noncoherent ultra-wideband receiver design," *IEEE Trans. Wireless Commun.*, vol. 10, no. 2, pp. 710–720, Feb. 2011.

[9] M. E. Sahin, I. Guvenc, and H. Arslan, "Optimization of energy detector receivers for UWB systems," in *Proc. IEEE Vehicular Technology Conference, Dallas USA*, vol. 2, June 2005, pp. 1386 – 1390.

[10] T. L. Marzetta and B. M. Hochwald, "Capacity of a mobile multiple-antenna communication link in Rayleigh flat fading," *IEEE Trans. Inform. Theory*, vol. 45, no. 1, pp. 139–157, Jan. 1999.

[11] B. M. Hochwald and W. Sweldens, "Differential unitary space-time modulation," *IEEE Trans. Commun.*, vol. 48, no. 12, pp. 2041–2052, Dec. 2000.

[12] B. L. Hughes, "Differential space-time modulation," *IEEE Trans. Inform. Theory*, vol. 46, no. 7, pp. 2567–2578, Nov. 2000.

[13] B. Hassibi and B. M. Hochwald, "Cayley differential unitary space-time codes," *IEEE Trans. Inform. Theory*, vol. 48, no. 6, pp. 1485–1503, June 2002.

[14] F. Oggier, "Cyclic algebras for noncoherent differential space-time coding," *IEEE Trans. Inform. Theory*, vol. 53, no. 9, pp. 3053–3065, Sep. 2007.

[15] X. Liang and X. Xia, "Unitary signal constellations for differential space-time modulation with two transmit antennas: parametric codes, optimal designs, and bounds," *IEEE Trans. Inform. Theory*, vol. 48, no. 8, pp. 2291 – 2322, Aug. 2002.

[16] D. Smith and L. Hanlen, "New group product differential unitary space-time codes with simplified design and detection," *IEEE Trans. Wireless Commun.*, vol. 7, no. 12, pp. 4825 – 4830, Dec. 2008.

[17] M. Bhatnagar, A. Hjorungnes, and L. Song, "Differential coding for non-orthogonal space-time block codes with non-unitary constellations over arbitrarily correlated Rayleigh channels," *IEEE Trans. Wireless Commun.*, vol. 8, no. 8, pp. 3985 – 3995, Aug. 2009.

[18] C. Abou-Rjeily and J.-C. Belfiore, "On space-time coding with pulse position and amplitude modulations for time-hopping ultra-wideband systems," *IEEE Trans. Inform. Theory*, vol. 53, no. 7, pp. 2490–2509, July 2007.

[19] C. Abou-Rjeily and W. Fawaz, "Space-time codes for MIMO ultra-wideband communications and MIMO free-space optical communications with PPM," *IEEE J. Select. Areas Commun.*, vol. 26, no. 6, pp. 938–947, Aug. 2008.

[20] R. Vehkalahti, "The coding gain of real matrix lattices: bounds and existence results," *IEEE Trans. Inform. Theory*, vol. 56, no. 9, pp. 4359–4366, Sep. 2010.

[21] C. Abou-Rjeily, N. Daniele, and J.-C. Belfiore, "Differential space-time ultra-wideband communications," in *Proc. IEEE Int. Conf. on Ultra-Wideband, Zurich Switzerland*, Sep. 2005, pp. 248–253.

[22] C. Abou-Rjeily, "Unitary space-time pulse position modulation for differential unipolar MIMO IR-UWB communications," *IEEE Trans. Wireless Commun.*, vol. 14, no. 10, pp. 5602–5615, Oct. 2015.

[23] Q. Zhang and C. S. Ng, "Differential space-time coded impulse radio systems using MIMO autocorrelation receivers in UWB channel," in *Proc. IEEE Int. Conf. on UWB, Boston USA*, Sep. 2006, pp. 441 – 446.

[24] ——, "DSTBC impulse radios with autocorrelation receiver in ISI-free UWB channels," *IEEE Trans. Wireless Commun.*, vol. 7, no. 3, pp. 806–811, Mar. 2008.

[25] T. Wang, T. Lv, H. Gao, and Y. Lu, "BER analysis of decision-feedback multiple-symbol detection in noncoherent MIMO ultrawideband systems," *IEEE Trans. Veh. Technol.*, vol. 62, no. 9, pp. 4684–4690, Nov. 2013.

[26] T. Wang, T. Lv, and H. Gao, "Sphere decoding based multiple symbol detection for differential space-time block coded ultra-wideband systems," *IEEE Commun. Lett.*, vol. 15, no. 3, pp. 269–271, Mar. 2011.

[27] L. Yang and G. B. Giannakis, "Analog space-time coding for multi-antenna ultra-wideband transmissions," *IEEE Trans. Commun.*, vol. 52, no. 3, pp. 507–517, Mar. 2004.

[28] S. M. Alamouti, "A simple transmit diversity technique for wireless communications," *IEEE J. Select. Areas Commun.*, vol. 16, no. 8, pp. 1451–1458, Oct. 1998.

[29] V. Tarokh, N. Seshadri, and A. Calderbank, "Space-time codes for high data rate wireless communication : Performance criterion and code construction," *IEEE Trans. Inform. Theory*, vol. 44, no. 2, pp. 744–765, Mar. 1998.

[30] J. Foerster, "Channel modeling sub-committee Report Final," Technical report IEEE 802.15-02/490, IEEE 802.15.3a WPANs, 2002.

[31] C. Abou-Rjeily, "Performance analysis of UWB systems over the IEEE 802.15.3a channel model," *IEEE Trans. Commun.*, vol. 59, no. 9, pp. 2377–2382, Sep. 2011.

[32] K. Maichalernnukul, T. Kaiser, and F. Zheng, "On the performance of coherent and noncoherent UWB detection systems using a relay with multiple antennas," *IEEE Trans. Wireless Commun.*, vol. 8, no. 7, pp. 3407 – 3414, July 2009.

[33] J. Kunisch and J. Pamp, "An ultra-wideband space-variant multipath indoor radio channel model," in *Proc. IEEE Conf. on UWB Systems and Technologies, Virginia USA*, Nov. 2003, pp. 290 – 294.